

ornl

ORNL/CON-359

**OAK RIDGE
NATIONAL
LABORATORY**

MARTIN MARIETTA

The Oak Ridge National Laboratory
Automobile Heat Pump Model:
User's Guide

D. M. Kyle

MANAGED BY
MARTIN MARIETTA ENERGY SYSTEMS, INC.
FOR THE UNITED STATES
DEPARTMENT OF ENERGY

**The Oak Ridge National Laboratory
Automobile Heat Pump Model:
User's Guide**

D. M. Kyle

Energy Division
Oak Ridge National Laboratory

May 1993

OAK RIDGE NATIONAL LABORATORY
Oak Ridge, Tennessee 37831-6285
managed by
MARTIN MARIETTA ENERGY SYSTEMS, INC.
for the
U. S. DEPARTMENT OF ENERGY
under Contract No. DE-AC05-84OR21400

10/10/10

10/10/10

10/10/10

10/10/10

10/10/10

CONTENTS

	<u>Page</u>
LIST OF FIGURES	v
ACKNOWLEDGEMENTS	vii
ABSTRACT	ix
1. INTRODUCTION	1
2. COMPONENT SUBMODELS	3
2.1 COMPRESSOR	3
2.2 FINNED-TUBE CONDENSER	6
2.3 EVAPORATOR	9
2.4 FLOW CONTROL DEVICES	12
2.5 EVAPORATOR PRESSURE REGULATOR	12
2.6 REFRIGERANT MASS	14
2.7 REFRIGERANT LINES	14
3. PROGRAM STRUCTURE	17
3.1 BASIC ALGORITHM	17
3.2 SOLUTION WHEN REFRIGERANT MASS IS SPECIFIED	19
4. VALIDATION	23
4.1 COMPONENT VALIDATION	23
4.2 SYSTEM VALIDATION	23
5. OVERVIEW OF PROGRAM USAGE	27
5.1 DESIGN/OPTIMIZATION STUDIES	27
5.2 SIMULATION STUDIES	27
5.3 MODEL AVAILABILITY AND SOFTWARE REQUIREMENTS	31
6. INPUT DATA FILE	33
6.1 TITLE AND CONTROL DATA	33
6.2 REFRIGERANT MASS DATA	35
6.3 EXPANSION DEVICE DATA	37
6.4 COMPRESSOR DATA	39
6.5 INDOOR HEAT EXCHANGER DATA	43
6.6 OUTDOOR UNIT DATA	49
6.7 REFRIGERANT LINES DATA:	52
6.8 SOLUTION CONVERGENCE CRITERIA :	54
7. SUMMARY	57
REFERENCES	59

APPENDIX A: DESCRIPTION OF SUBROUTINE CHANGES	63
APPENDIX B: INPUT AND OUTPUT FILES FOR COMPRESSOR CURVE-FITTING PROGRAM	73
APPENDIX C: SAMPLE AUTOMOBILE HEAT PUMP MODEL OUTPUT	83
APPENDIX D: DEFINITIONS OF CONSTANTS ASSIGNED IN BLOCK DATA	91

LIST OF FIGURES

	<u>Page</u>
Fig. 1. Schematic of a finned-tube heat exchanger with staggered tubes.	7
Fig. 2. Schematics of various refrigerant flow circuits.	8
Fig. 3. Plate-fin automotive air conditioning evaporator.	10
Fig. 4. Plate-fin heat exchanger geometry.	11
Fig. 5. Functional relation between the area of the valve opening and the inlet pressure, for a direct-acting evaporator pressure regulator.	13
Fig. 6. Flow chart showing basic solution algorithm. See text for explanation of symbols.	18
Fig. 7. Program control options when total refrigerant mass is specified.	21
Fig. 8. Comparison of plate-fin evaporator submodel with laboratory test measurements.	24
Fig. 9. Flow chart depicting recommended methodology for simulation studies using the Automobile Heat Pump Model.	28
Fig. 10. Sample input data file "HPDATA." Boxed data illustrate the changes in the structure of the data file that result from the choice of compressor submodel and of the indoor heat exchanger submodel.	34
Fig. 11. Schematic of an accumulator.	37
Fig. 12. Thermal expansion valve mass flow rate (or capacity). The variables shown correspond with the input variables on line 6 of the HPDATA.	39
Fig. 13. Plate fin geometry.	45
Fig. 14. Schematic drawings of finned-tube heat exchangers.	47

MEMORANDUM

TO : [Illegible]

FROM : [Illegible]

SUBJECT: [Illegible]

[Illegible text follows, consisting of several paragraphs of a memorandum format.]

ACKNOWLEDGEMENTS

The authors wish to thank Mr. P. Malone of Eaton Corporation for providing test data used for evaporator submodel validation. Thanks also to Mr. H. G. Stewart of Tecumseh Products Company for sharing automotive compressor data. We also thank Dr. C. K. Rice of Oak Ridge National Laboratory for his frequent and informative conversations during the code development. This work was a part of the Transportation Environmental Control activities at Oak Ridge National Laboratory sponsored by the Office of Transportation Technologies, U.S. Department of Energy, under contract DE-AC05-84OR21400 with Martin Marietta Energy Systems, Inc.

ABSTRACT

A computer program has been developed to predict the steady-state performance of vapor compression automobile air conditioners and heat pumps. The code is based on the residential heat pump model developed at Oak Ridge National Laboratory. Most calculations are based on fundamental physical principles, in conjunction with generalized correlations available in the research literature. Automobile air conditioning components that can be specified as inputs to the program include open and hermetic compressors; finned tube condensers; finned tube and plate-fin style evaporators; thermal expansion valve, capillary tube and short tube expansion devices; refrigerant mass; evaporator pressure regulator; and all interconnecting tubing. The program can be used with a variety of refrigerants, including R134a. Methodologies are discussed for using the model as a tool for designing all new systems or, alternatively, as a tool for simulating a known system for a variety of operating conditions.

1. INTRODUCTION

In recent years, several computer models for simulating the performance of residential heat pumps and air conditioners have been presented in the open literature (Hiller and Glicksman 1976; Ellison and Creswick 1978; Domanski and Didion 1983; Fischer and Rice 1983; Fadel 1988; Hill and Jeter 1991). Computer models for *automobile air conditioners* so far have not been made available to the public, however. To fill this void, we have developed an automobile heat pump model (AHPM) based upon the variable-speed residential heat pump model that was developed at Oak Ridge National Laboratory (ORNL) (Rice and Fischer 1985; Rice 1988; Rice 1992). Several new component submodels have been added to the residential heat pump model to simulate automobile air conditioning and heat pump systems. These include belt-driven open compressors, plate-fin style evaporator coils, and an evaporator pressure regulator. Also, evaporator and condenser fans are specified in a way that is suitable for automotive applications. In general, modifications have been restricted to the use of mathematical correlations that exist in the open literature. Altogether, 20 new or modified FORTRAN subroutines have been added to the residential heat pump model to create the AHPM. These changes will be described in the following pages in more detail.

This report is intended primarily as a self-contained guide for users unfamiliar with any of the previous versions of the ORNL residential heat pump model. For this reason, the description of the submodels for each system component (Sect. 2) includes a *physical* description of the configurations that can be handled by the program. In Sect. 3, the solution algorithm is briefly described to enable the user to understand how the major components are used together within the program. Component level and system level validation are described in Sect. 4. A methodology for using the code in system simulation activities is described in detail in Sect. 5. A line-by-line description of the input data file for the AHPM is given in Sect. 6.

1911

The first part of the year was spent in the
 study of the history of the country and
 the progress of the various industries.
 The second part was devoted to the
 study of the natural history of the
 country and the progress of the
 various industries. The third part
 was devoted to the study of the
 natural history of the country and
 the progress of the various industries.
 The fourth part was devoted to the
 study of the natural history of the
 country and the progress of the
 various industries. The fifth part
 was devoted to the study of the
 natural history of the country and
 the progress of the various industries.
 The sixth part was devoted to the
 study of the natural history of the
 country and the progress of the
 various industries. The seventh part
 was devoted to the study of the
 natural history of the country and
 the progress of the various industries.
 The eighth part was devoted to the
 study of the natural history of the
 country and the progress of the
 various industries. The ninth part
 was devoted to the study of the
 natural history of the country and
 the progress of the various industries.
 The tenth part was devoted to the
 study of the natural history of the
 country and the progress of the
 various industries.

2. COMPONENT SUBMODELS

The submodels for each of the system components are described in this section. They are intended to help the user understand exactly what types of components can be simulated accurately. Important information concerning the submodels is also found in the residential heat pump model documentation (see Fischer and Rice 1983; Fischer, Rice, and Jackson 1988; and Rice 1991). Detailed information concerning changes to the FORTRAN source code that have been made while developing the AHPM is given in Appendix A.

2.1 COMPRESSOR

Belt-driven open compressors are used in virtually all currently installed automobile air conditioning systems. In internal combustion engine vehicles, this prevalence is not expected to change in the near future. For this reason, submodels for open compressors are described first. The two open compressor submodels that will be described are actually modifications of two analogous submodels found in the residential heat pump version, which simulate electrically driven *hermetic* compressors. The hermetic submodels are available in the AHPM as well, where they are of potential use for designing heat pump and air conditioner systems for electric and hybrid vehicles. The subprograms can be used to describe any positive displacement compressor, whether open or hermetic, including reciprocating, scroll, vane, and rolling piston compressors.

Both of the open compressor submodels calculate mass flow rate, compressor shaft power, and the refrigerant enthalpy at the exit. These performance variables are evaluated using three independent variables: superheat and suction pressure at the inlet, and the discharge pressure. In addition to these three independent variables, the submodels also require a description of how a particular compressor performs. To describe the compressor performance, the AHPM user is *not* required to describe in detail the mechanical design itself, beyond specifying the shaft speed and total displacement. Instead, the user characterizes the mechanical performance by specifying the volumetric and isentropic efficiencies and the rate of heat release from the compressor shell. The two open compressor submodels differ in how the user will specify these efficiencies.

Variable-speed submodel—To study the system behavior over a range of shaft speeds, the user is first required to obtain performance data—either from calorimeter tests or from

the manufacturer—specifying \dot{m} and shaft power as a function of the suction pressure and discharge pressures, for several shaft speeds. The user inputs these data into a stand-alone curve-fitting program provided with the AHPM. A description of how to use this program is provided in Appendix B. The curve-fitting program produces the coefficients from a least-squares polynomial fit to the data. Once these coefficients are inserted into the input file for the AHPM, description of the variable-speed compressor performance is complete.

The compressor subprogram uses the curve-fit coefficients to derive the isentropic and volumetric efficiencies. The definition of isentropic efficiency η_{isen} used throughout this report is

$$\eta_{isen} = \frac{\dot{m}(h_{isen} - h_{in})}{\text{shaft power}}, \quad (1)$$

where

h_{in} is the enthalpy of the refrigerant entering the compressor,

h_{isen} is the exiting refrigerant enthalpy that would result from a reversible compression process,

\dot{m} is the mass flow rate of refrigerant.

The shell heat loss is described using a “thermal efficiency,” η_{therm} . The user must specify the thermal efficiency η_{therm} as a quadratic function of the condensing temperature t_{cond} :

$$\eta_{therm} = a_1 + a_2 T_{cond} + a_3 T_{cond}^2, \quad (2)$$

where $a_{1,2,3}$ are arbitrary constants. η_{therm} is defined as

$$\eta_{therm} = \frac{\dot{m}(h_{out} - h_{in})}{\text{shaft power}}, \quad (3)$$

where h is the enthalpy exiting the compressor.

The variable speed model allows the user to simulate the behavior of a particular compressor essentially to within the degree of accuracy of the empirical performance data. It is useful for studying the *system performance over a wide range of pressures and shaft*

speeds. If compressor data are not available to the user, then sample coefficients are provided. These coefficients are found in Appendix B and on the floppy disk sent out with the AHPM. The coefficients were obtained from data that were provided to ORNL by a major automotive compressor manufacturer.

Often a manufacturer produces a *series* of similar compressor models, all with similar components but with different displacements. The AHPM user is free to vary the displacement while using a single set of performance curves. The submodel calculates the volumetric and isentropic efficiencies using the curves, together with the specified displacement to calculate the performance variables mentioned above. In this way, *the submodel can be used for predicting the system performance for a variety of compressors having different displacements, assuming that they are all mechanically similar.*

Explicit efficiency submodel—In the second type of open compressor submodel, the user specifies the isentropic efficiency explicitly as a *constant*, thus ignoring its strong dependence on compressor speed. The volumetric efficiency either is specified as a constant or can be calculated automatically using an internally supplied function of the pressure ratio (for details of this function, see Fischer and Rice 1983). The thermal efficiency is specified as described earlier. *This submodel is useful for examining the system performance as a function of the compressor efficiencies, at a single shaft speed.* This submodel may be of interest to the user whose primary interest is in studying the effects of novel compressors or compressors not well represented by the curve fits provided.

It is very important to note that in real compressors, the isentropic and volumetric efficiencies are definite functions of both shaft speed and pressure ratio. This submodel is for a single speed only. The pressure ratio dependence requires further discussion, however. Again, in a real system as, for example, the inlet air temperature changes, the pressure ratio also changes. In turn, the isentropic efficiency will change.

In contrast, the user of the explicit efficiency submodel who decides to examine the effect of changing inlet air temperature (or any other parameter) has artificially *fixed* the isentropic efficiency value. A natural question is: If one of the system parameters is changed, can the user of the explicit efficiency submodel regard the resulting changes in overall system performance as reflecting the true system dependence upon that parameter? The answer is yes, but only if changes that simultaneously occur in the *pressure ratio are small*. If changes in the pressure ratio are small, then the pressure ratio dependence of the volumetric efficiency is adequately described by the internal function mentioned above, while the pressure ratio dependence of the isentropic efficiency often can be regarded as only a weak function of pressure ratio at moderate pressure ratios.

Hermetic compressors— For hermetic compressors, the user specifies electric frequency in order to characterize the compressor speed, as opposed to the shaft speed. The hermetic submodels also include built-in speed-torque-efficiency relations for various motor types (e.g., inverter driven ac induction motors and electronically commutated dc motors), enabling the user to examine the overall system effect of choosing different motor technologies. These subprograms are not documented in this report, but they are described by Rice (1991).

2.2 FINNED-TUBE CONDENSER

The condenser submodel used in the residential model (Fischer and Rice 1983; Rice 1991) has been retained in the AHPM without modification. The submodel is composed of mathematical correlations that were chosen for simulating an air-cooled, cross-flow, finned-tube heat exchanger with staggered round tubes (Fig. 1). Note that although this condenser configuration is widely used in American cars, many cars are equipped with condensers having "corrugated" air-side fins and/or flattened refrigerant tubes, either in a serpentine configuration or in crossflow between two side headers. General correlations for flat-tube condensers were not available in the literature and therefore are not included.

The AHPM user can specify the finned-tube condenser geometry in considerable detail. Physical parameters that the user selects include fin thickness, fin pitch, horizontal and vertical tube spacing, and tube diameters. Air-side correlations include the effects of fin patterns used for heat transfer enhancement. For example, correlations developed for ORNL by Beecher and Fagan (1987) can be used for wavy and zigzag fin patterns.

The submodel can predict the condenser performance for a variety of refrigerant tube circuiting arrangements. One such arrangement is depicted in Fig. 2a. Notice that in this case, after the incoming refrigerant is split into three parallel streams, each of the streams traverses the width of the heat exchanger only once at the top tier, after which each stream is diverted through a return bend to the next lowest tier, where it once again traverses the width of the condenser. This type of flow is called "single pass." In contrast

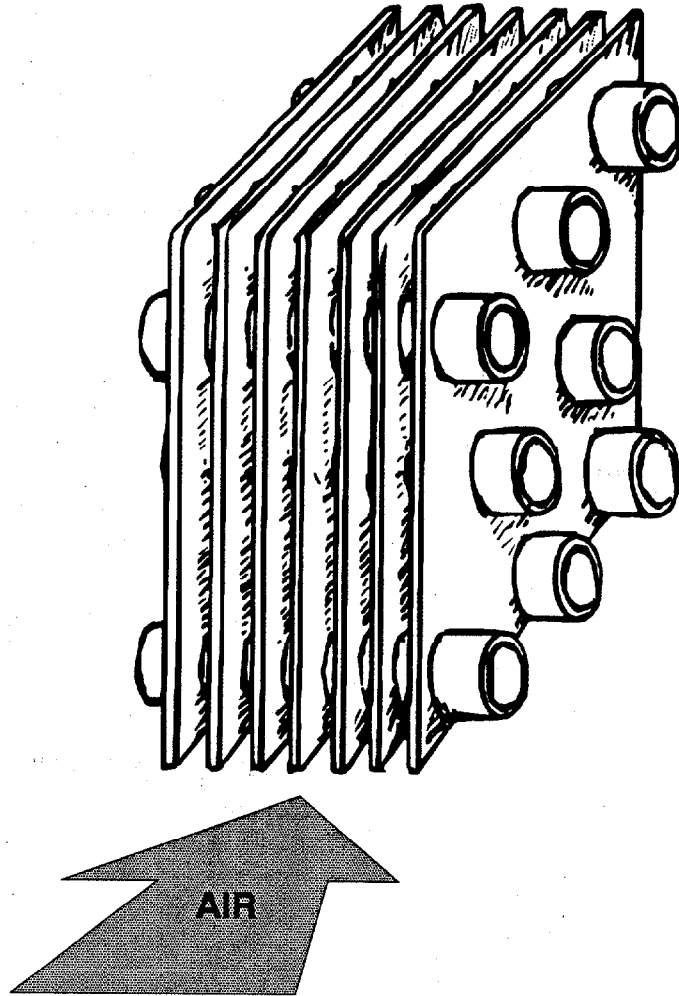
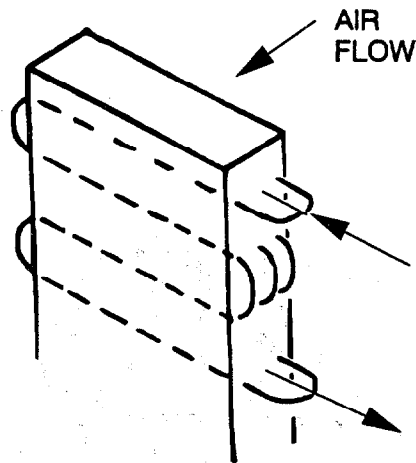
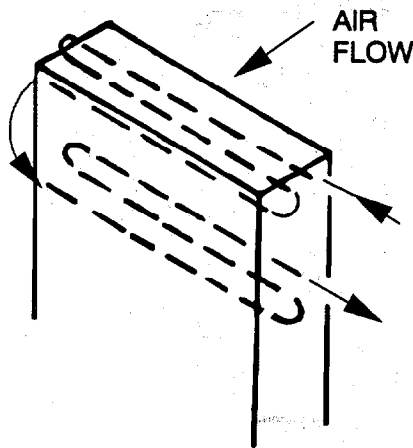


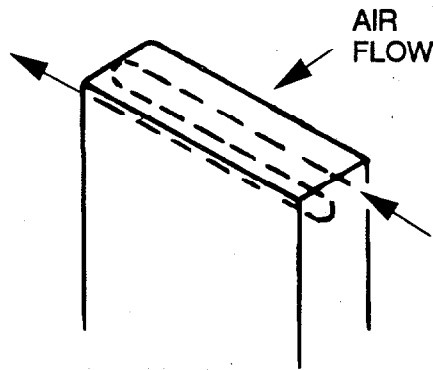
Fig. 1. Schematic of a finned-tube heat exchanger with staggered tubes.



(a.) Single pass



(b.) Multi-pass — with initial and final passes on leading edge of coil



(c.) Multi-pass — with final pass on trailing edge of coil

Fig. 2. Schematics of various refrigerant flow circuits. *Source:* adapted from Hiller, C.C., and L. R. Glicksman 1976. "Improving Heat Pump Performance via Compressor Capacity Control—Analysis and Test, Vols. I and II," Massachusetts Institute of Technology Energy Laboratory Report MIT-EL 76-001, Cambridge, Mass.

to single-pass flow, Fig. 2b depicts a refrigerant stream that traverses the heat exchanger three times in the same tier before being diverted to a lower tier. When multiple passes occur in a single tier, the circuiting is termed "multipass."

The finned-tube condenser submodel in the AHPM is valid for all single-pass flows. However, only certain multipass flows are accurately simulated by the submodel. In multipass arrangements that are well represented by the submodel, the single-phase vapor flow is not behind (in the direction of air streaming) the two-phase refrigerant flow, and the single-phase liquid flow also is not behind the two-phase flow. For the case depicted in Fig. 2b, refrigerant in the top tier is near the front face of the coil where air enters. Therefore, whether the refrigerant enters as superheated vapor or as saturated liquid, a single-phase flow is not behind a two-phase flow. In the second tier, any single-phase liquid flow is in front of, not behind, the two-phase flow. Thus, the arrangement shown in Fig. 2b is accurately modeled, and the arrangement shown in Fig. 2c is not.

A full discussion of these issues is given by Hiller and Glicksman (1976), whose submodel has been followed closely here. This submodel relies upon the "effectiveness/thermal units" technique developed by Kays and London (1974). The algorithm automatically calculates the fraction of the heat exchanger that is dedicated to single-phase vapor, single-phase liquid, and two-phase flow. The thermal performance of each area is reported individually as part of the standard AHPM output (see Appendix C).

2.3 EVAPORATOR

By far the most common configuration for evaporators installed in domestic and foreign automobiles is the air-cooled, cross-flow, plate-fin heat exchanger with louvered, corrugated-style air fins. A typical automobile plate-fin evaporator configuration is pictured in Fig. 3. This type of heat exchanger has air fins sandwiched between parallel plates. The plates separate the air stream from the refrigerant stream in alternating stacked layers (Fig. 3). The refrigerant passages are connected in parallel by suitable headers to form the two sides of the exchanger. Substantial code alterations have been made to the residential heat pump version to enable AHPM users to include these types of evaporators in their studies. These code changes, including the mathematical correlations for simulating automobile plate-fin evaporators, are described in Appendix A.

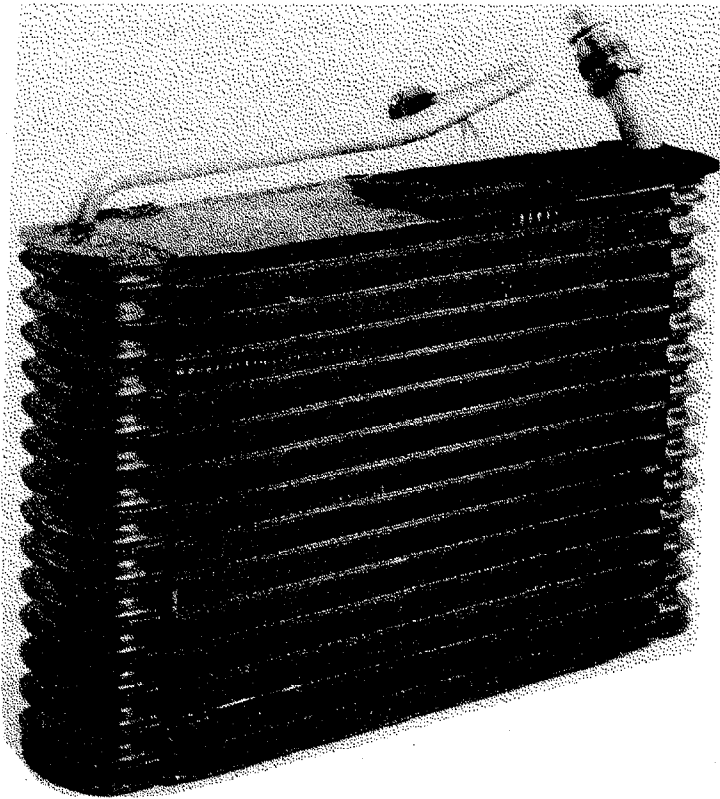


Fig. 3. Plate-fin automotive air conditioning evaporator.

The air-side fins are typically made in the “corrugated” pattern shown in Fig. 4a. The fins used in automotive evaporators typically are stamped so as to create a louvered surface (Fig. 4a). When the fins are inserted, they form individual flow passages, as shown in Fig. 4b. On the other hand, the flow on the refrigerant side often is not channeled at all. In fact, the plates are embossed with patterns designed to facilitate full mixing in the direction normal to the refrigerant flow. The AHPM user specifies physical parameters for describing these geometric features in considerable detail. Parameters include louver width, fin pitch, and fin thickness and, on the refrigerant side, plate thickness and details related to the rib pattern shown in Fig. 4b. The discussion in Sect. 3.2 related to single-pass and multipass flow arrangements pertains here as well; however, note that virtually all automobile plate-fin evaporators have single-pass designs.

The *finned-tube* style evaporator submodel used in the residential version has also been retained for use in the AHPM. In fact, users *must* select this configuration for studying any *heat pump* designs, for example, for electric vehicles. The reason is that no correlations for condensation in plate-fin heat exchangers of the type used in automobiles was found in the literature. If the AHPM user wishes to design an indoor heat exchanger that serves as both an evaporator and a condenser, he or she is confined to modeling a finned-tube design.

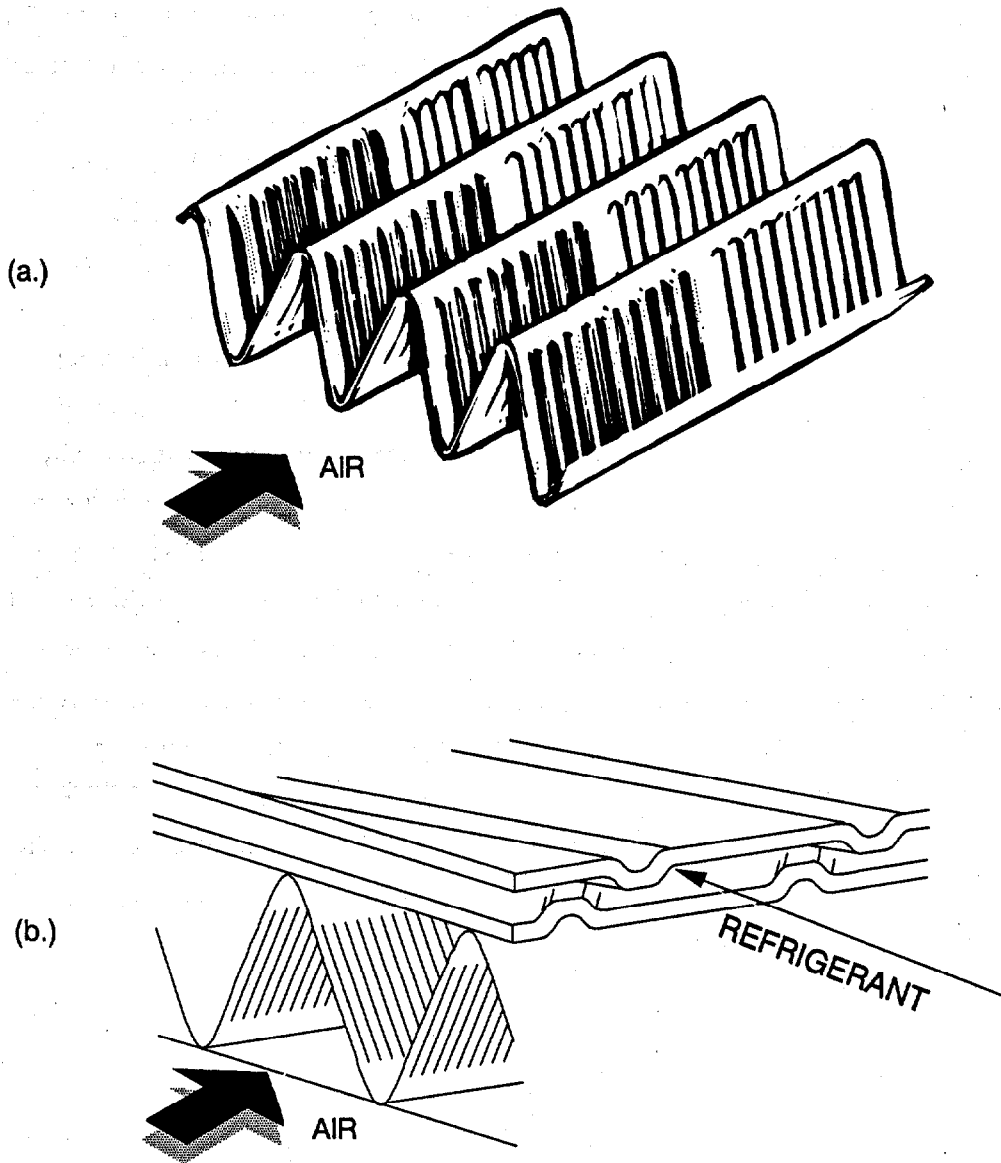


Fig. 4. Plate-fin heat exchanger geometry. (a) Shows "corrugated" fins having slits or louvers that are regularly spaced in the direction of air flow. (b) Shows how corrugated air fins are sandwiched between plates to form a cross-flow heat exchanger.

2.4 FLOW CONTROL DEVICES

The AHPM contains subroutines for one or more capillary tubes, a short-tube orifice, and a cross-charged thermal expansion valve (TXV).¹ The capillary tube submodel uses the empirically obtained curves given in the ASHRAE Equipment Handbook (1988). The short tube calculations use empirical correlations developed by Mei (1982). Mei obtained data for a variety of long "accurators" manufactured by Carrier Corporation for several orifice diameters and length-to-diameter ratios. The TXV submodel uses the algorithm described by Fischer and Rice (1983) and Fischer, Rice, and Jackson (1988). The user inputs parameters directly related to the physical dimensions of the device in the case of the capillary tubes and short-tube. In the case of the TXV, the user must specify performance-related parameters that typically are provided by the TXV manufacturer.

Regarding the limitations of the expansion device subprograms, note first that the mathematical correlations for the capillary tube involve coefficients derived specifically for use with R-12 and R-22. Recent experimental results by Wijaya (1991) suggest that these correlations should describe capillary flow for R-134a to within a 5% error. Mei's short-tube correlations pertain strictly to R-22. No data are available for comparing these results with results for other refrigerants. The refrigerant dependence of the TXV correlations is not an issue because the TXV performance data provided by manufacturers always relates to a specific TXV model used with a specific refrigerant. Finally, note an important limitation of all three devices: In cases where two-phase flow enters the expansion device, the accuracy of the submodels suffers. If this occurs, the AHPM completes execution, but the results are inaccurate. The user must always examine the output to ensure that the refrigerant entering the expansion device is subcooled.

2.5 EVAPORATOR PRESSURE REGULATOR

Many automobile air conditioning systems use an evaporator pressure regulator (EPR). The device is installed into the suction line to maintain a fixed minimum evaporator pressure to prevent coil freezing. Unfortunately, the valve causes pressure in the suction line to drop further, which can significantly reduce the system efficiency, as

¹A "cross-charged" TXV is one in which the temperature sensing bulb is filled with a liquid that is different from the system refrigerant. Cross-charged TXVs are commonly used and provide for a more constant evaporator superheat over a wide range of evaporating temperatures.

well as reduce maximum capacity. The capability for modeling an EPR has been added to the AHPM. It is intended to enable system designers to select those EPR characteristics that lead to optimal system performance over the anticipated range of operating conditions.

The direct-acting pressure regulator is modeled using the relation

$$\dot{m} = C_{EPR} A \sqrt{\rho(P_{in} - P_{out})} , \quad (4)$$

where

A represents the area of the valve opening,

C_{EPR} is a constant,

ρ is the density of the refrigerant vapor,

P_{in} and P_{out} are the refrigerant pressures of the valve inlet and outlet, respectively.

For evaporator pressure regulators, A is characteristically a function of the inlet pressure P_{in} alone (ASHRAE 1988). The assumed functional relation between A and P_{in} is shown in Fig. 5. The user is free to specify $P_{in,min}$, $P_{in,rated}$, $A(rated)$ and C_{EPR} .

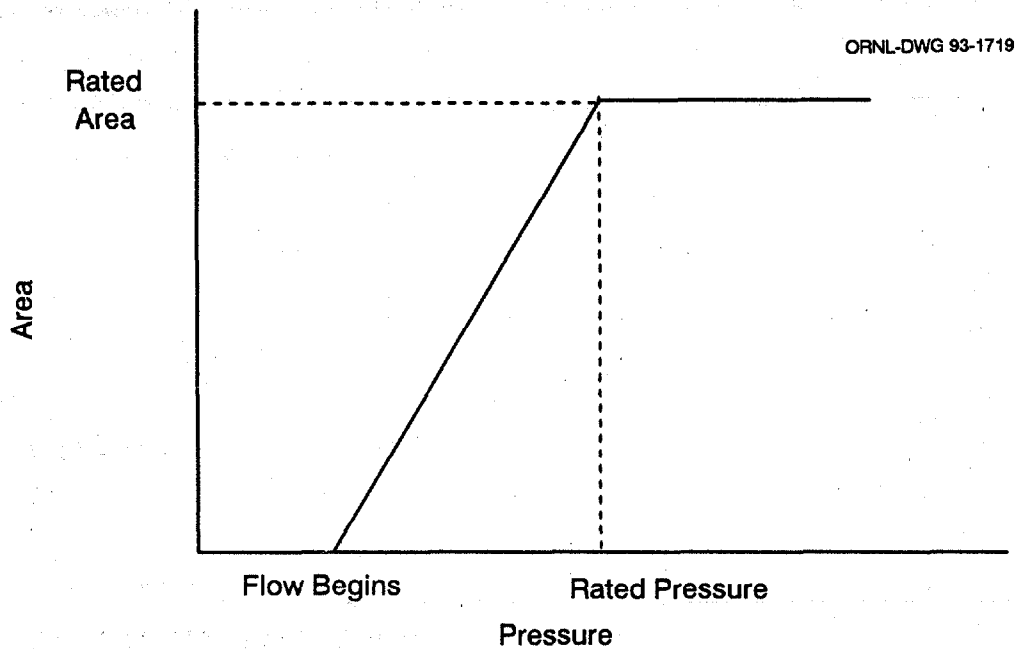


Fig. 5. Functional relation between the area of the valve opening and the inlet pressure, for a direct-acting evaporator pressure regulator.

Regarding the program execution, Eq. 4 is used in the following way. When the compressor subroutine is called, pressure at the compressor inlet—which is P_{out} in Eq. 4—is treated as fixed, along with discharge pressure and suction superheat. First, \dot{m} is calculated. Then, at the end of the subroutine, the pressure drop in the suction line is calculated, using \dot{m} . It is at this point that Eq. 4 is used to find P_{in} as a function of \dot{m} and P_{out} .

2.6 REFRIGERANT MASS

The AHPM users have the option of calculating the refrigerant mass that resides in each of the system components. The mass calculation submodel has been developed by Rice (1987, 1991). It includes a choice of mass calculation methods. Details of these methods are found in Rice (1987). It also includes a j-tube accumulator model adapted from work at the National Institute of Science and Technology (Domanski and Didion 1983) for determining how much refrigerant is stored in the accumulator, if an accumulator is specified. The mass calculation submodel provides the designer with feedback on how various heat exchanger size options and various refrigerant control options affect the mass requirements at some fixed operating condition. Perhaps even more important, calculating the mass in each component is an integral part in the control logic that enables the AHPM user to *specify* the refrigerant mass as an initial condition, and to *study the variations in system performance as that mass redistributes itself for various operating conditions* (see Sect. 3.2).

2.7 REFRIGERANT LINES

The AHPM user specifies the dimensions of all refrigerant lines. Pressure drop in each line is calculated from correlations for single-phase flow and for two-phase flow. The correlations have been documented by Fischer and Rice (1983).

Heat transfer from refrigerant lines has been identified (Diekmann 1992) as a potential design improvement potential for automobile systems. In the AHPM, heat losses or gains in the suction and discharge lines are specified as constants and are not computed as a part of the solution.

In *heat pump* studies, the function of the reversing valve of redirecting flow is simulated automatically when the user selects either heating or cooling mode. The

pressure losses associated with refrigerant flow through the valve are *not modeled*.

Estimates of the typical system performance error incurred by neglecting reversing valve losses have been made by Krishnan (1986) and in a survey paper by Damasceno, Rooke, and Goldschmidt (1991). Krishnan found system losses ranging from 4.0 to 5.5% in system capacity and 4.0 to 6.0% in efficiency using three valve brands in a typical residential heat pump. Damasceno computed system losses for three valves averaging 2.5% in capacity and 1.7% in efficiency in cooling mode, and 2.1% in capacity and 3.4% in efficiency in heating mode.

1870
The first of the year was a very cold one, and the
frost was very early. The snow was very deep,
and the wind was very high. The weather was
very bad, and the people were very
suffering. The crops were very poor,
and the people were very poor.
The year was a very bad one,
and the people were very poor.

3. PROGRAM STRUCTURE

3.1 BASIC ALGORITHM

Following the flow chart in Fig. 6, the compressor submodel first calculates refrigerant mass flow rate \dot{m}^c and the exiting refrigerant enthalpy as functions of the inlet superheat and of the current suction and discharge pressure estimates. The condenser submodel then calculates the refrigerant state leaving the condenser as a function of both the entering refrigerant state, \dot{m}_c , and the air stream properties. The selected expansion device submodels (TXV, short tube, or capillary tube) then use their entering refrigerant state and the current suction pressure estimate to calculate a mass flow rate \dot{m}_f through the expansion device, independent of \dot{m}_c . As shown in Fig. 1, it is at this juncture that the compressor discharge pressure is adjusted: The error ($\dot{m}_f - \dot{m}_c$) is used in a simple Newton-Raphson routine to evaluate an improved discharge pressure estimate. Note that the pressure drop and the heat exchanged along the interconnecting tubing are accounted for explicitly in the program. Also, the suction pressure is used in the flow control subprogram as the pressure exiting the control device. This assumption is improved upon later, once all the low-side pressure drops have been calculated.

The user can omit specifying the expansion device. In this case, the system of equations making up the model becomes incomplete or "undetermined." To correct for this situation, the user must specify the subcooling at the condenser exit. In this case, the iteration loop shown in Fig. 6 adjusts compressor discharge pressure just as with the expansion device. The difference is that the expansion device subroutine is not used to calculate \dot{m}_f . Of course, the convergence criterion can no longer be to minimize ($\dot{m}_f - \dot{m}_c$). Instead, the subcooling calculated in the condenser routine, $\Delta T_{SC,calc}$, is used directly in a new convergence criterion, which is to minimize ($\Delta T_{SC,calc} - \Delta T_{SC,spec}$). The expansion device subroutines *are* used, but only to calculate the size of the device that would be appropriate *given* the compressor mass flow rate \dot{m}_c and $\Delta T_{SC,calc}$. This option is used as an intermediate step in the methodology described in Sect. 5 for obtaining the most accurate heat pump simulation possible. Apart from that role, this option could also serve as the physically correct choice for modeling an expansion device that adjusts automatically to regulate the subcooling at the condenser exit, analogous to an idealized TXV that adjusts to maintain a constant refrigerant superheat at the evaporator exit.

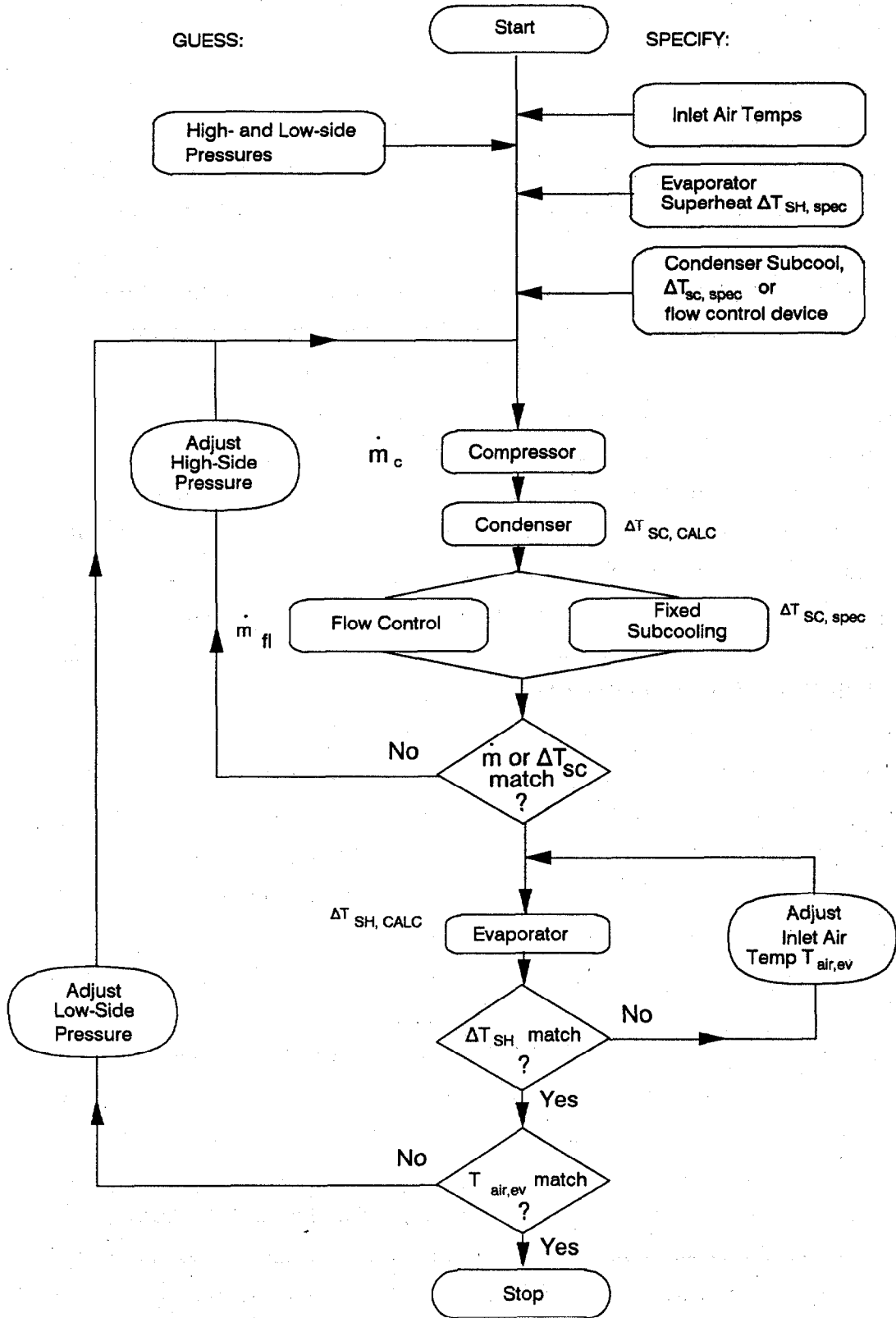


Fig. 6. Flow chart showing basic solution algorithm. See text for explanation of symbols.

When m_f and m_c (or $\Delta T_{SC,calc}$ and $\Delta T_{SC,spec}$) match to within a specified tolerance, then the algorithm enters the evaporator subprogram. When the mass flow rates m_f and m_c (or $\Delta T_{SC,calc} - \Delta T_{SC,spec}$) match to within a specified tolerance, then the algorithm enters the evaporator subprogram. To understand what is required of the evaporator submodel, note that for any evaporator, *five* boundary conditions are needed to characterize the refrigerant stream completely (e.g., inlet pressure, inlet enthalpy, outlet pressure, outlet enthalpy, and mass flow rate). It turns out that as a general principle, any *three* can be fixed independently, while the remaining two are then determined automatically. The three independent variables used in the evaporator submodel are—at the inlet—the enthalpy leaving the expansion device and the mass flow rate and—at the outlet—the current estimate of suction pressure (minus suction line losses). The two *dependent* variables that the submodel calculates are the incoming pressure and the outgoing superheat (or quality). The difference between the newly evaluated evaporator superheat and the user-specified value ($\Delta T_{SH,calc} - \Delta T_{SH,spec}$) is used in a Newton-Raphson scheme to search for the incoming evaporator air temperature that will minimize ($\Delta T_{SH,calc} - \Delta T_{SH,spec}$). When this difference is small enough, the algorithm compares the derived value for evaporator inlet air temperature with the user-specified entering air temperature. This comparison is used to adjust the suction pressure. When both $\Delta T_{SH,calc}$ and evaporator air temperature match the user-specified values, then the system is solved. Note that although the difference ($\Delta T_{SH,calc} - \Delta T_{SH,spec}$) could have been used to adjust the suction pressure directly, the present scheme involving another iteration on evaporator air temperature has been found to yield a more stable algorithm.

3.2 SOLUTION WHEN REFRIGERANT MASS IS SPECIFIED

The basic algorithm depicted in Fig. 6 requires that the user specify the refrigerant superheat at the compressor inlet. In reality, the refrigerant state at any point in a *system* is determined by the system design and the operating conditions, and it cannot be fixed by the person operating the system. The reason that the superheat must be fixed within the basic algorithm (Fig. 6) is that the refrigerant mass is not assigned. The refrigerant mass is a system component like any other, and it has a significant impact on performance. When the mass is unspecified in the system of equations making up the model, the model is underdetermined and requires an additional constraint (superheat) to arrive at a unique solution.

A key feature of both the residential heat pump version and the AHPM is that they allow users to specify the refrigerant mass. From a computational perspective, this is done by adding an outermost iterative loop in the heat pump solution scheme, as depicted in Fig. 7a. The program will iteratively adjust the evaporator superheat and repeat the basic algorithm depicted in Fig. 6 until the masses stored in the individual components add up to equal the specified total (Fig. 7a). Users thus can predict the *overall system effects of a given charge level as operating conditions are varied*. This enables more realistic off-design predictions as, for example, more and more refrigerant accumulates in the condenser coil. Alternatively, at a single operating condition, *the refrigerant mass values at which over- and undercharging effects begin to occur can be determined*. Overcharging is characterized by excessive subcooling or a flooded evaporator. Undercharging is characterized by zero subcooling.

Finally, the AHPM user may simply omit the expansion device from the hardware description but include the refrigerant charge. Analytically, omitting one of the system components, in this case the expansion device, requires that one other constraint be specified, which has been chosen to be the compressor suction superheat. The solution method for this option is shown in Fig. 7b. In this case, the program will iteratively adjust the condenser exit subcooling in the outermost loop and repeat the basic algorithm with the subcooling fixed (see the dotted lines in Fig. 6). Again, this is repeated until the masses stored in the individual components add up to equal the specified total. The usefulness of this option is the subject of Sect. 5.2.

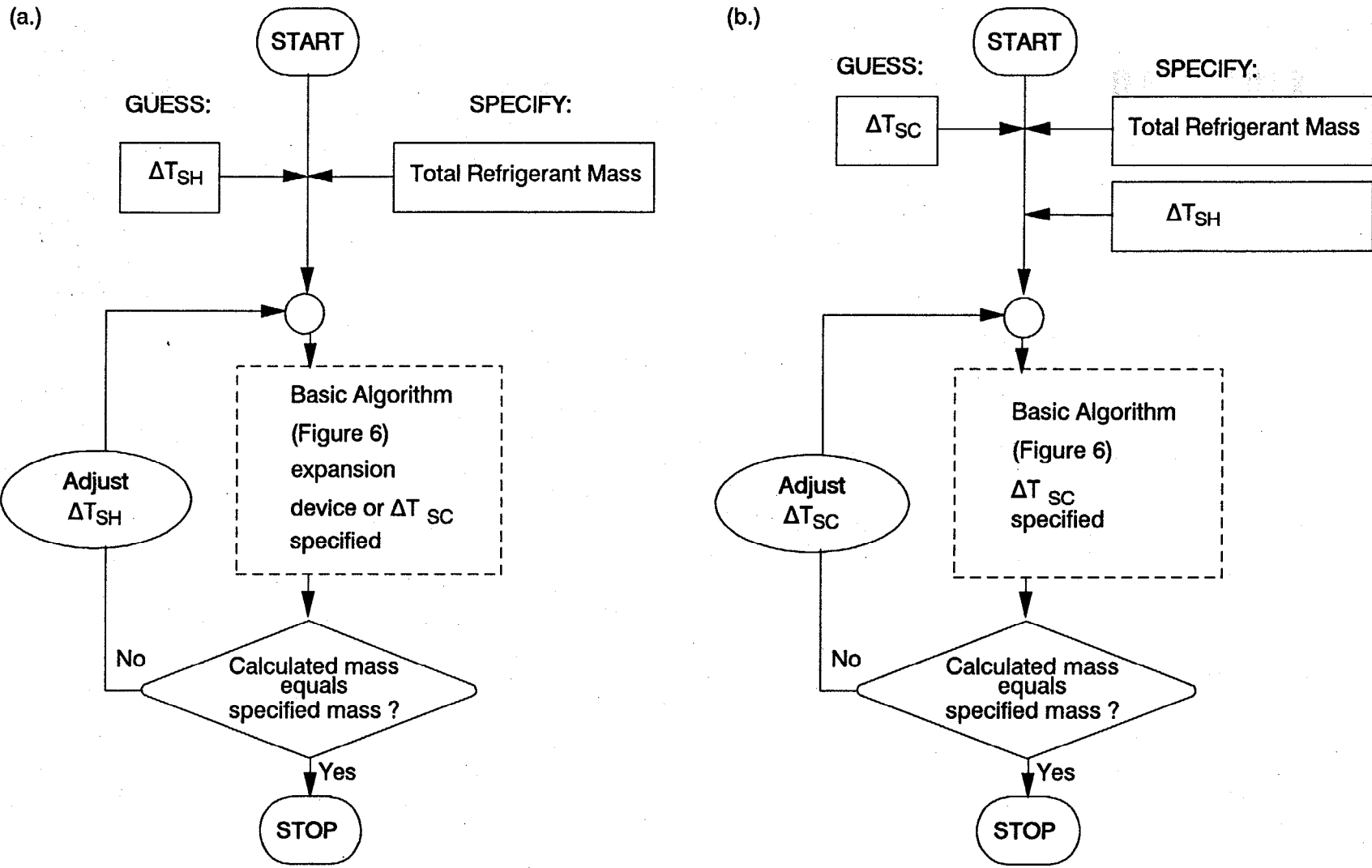
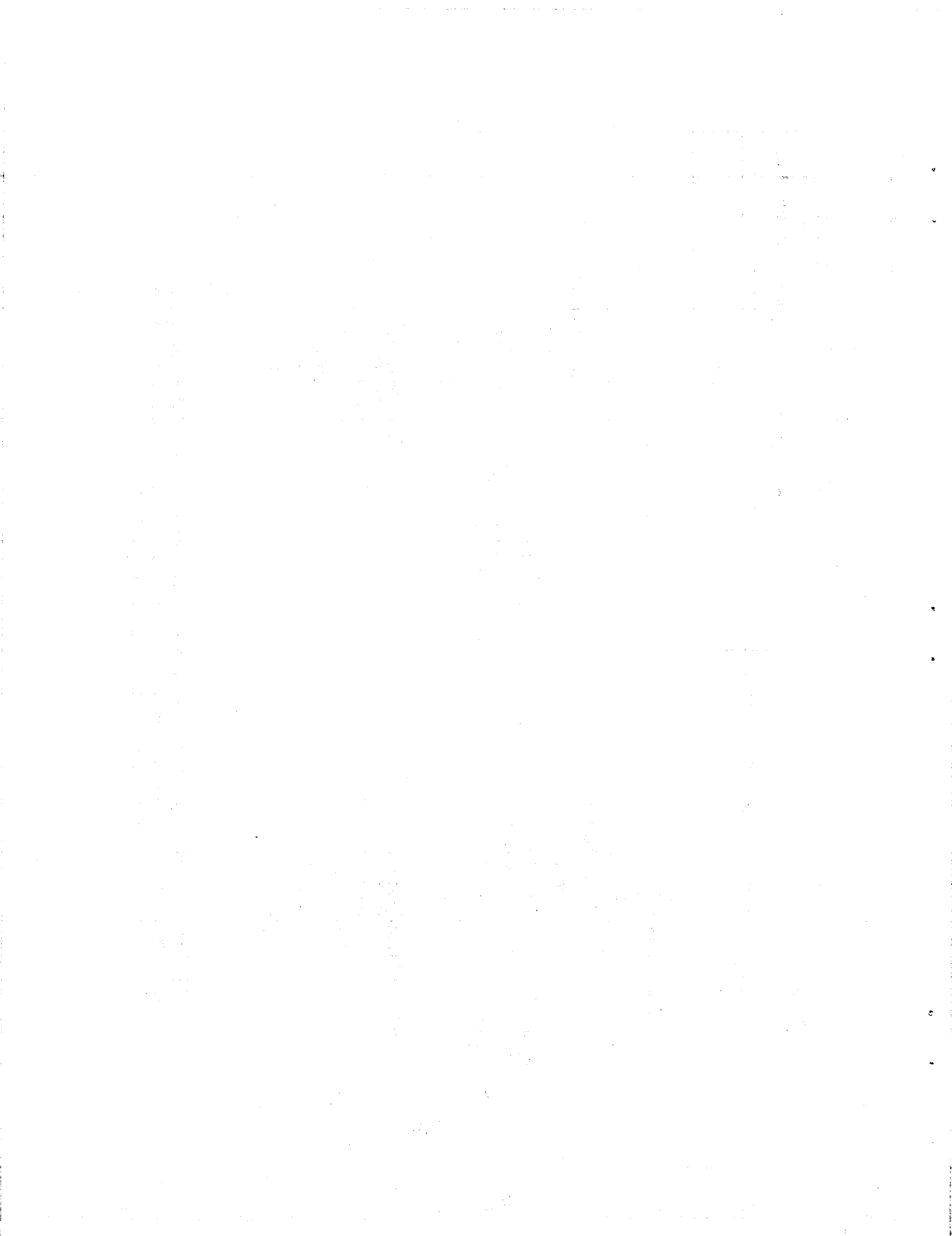


Fig. 7. Program control options when total refrigerant mass is specified. (a) When the expansion device is specified, the refrigerant temperature is calculated everywhere in the system. (b) When the expansion device is not specified, suction superheat ΔT_{sh} is fixed.



4. VALIDATION

4.1 COMPONENT VALIDATION

Validation of the new plate-fin evaporator submodel has been carried out using performance data obtained through a cooperative agreement with a major component manufacturer. Laboratory tests were conducted over a wide range of conditions comprising three compressor speeds (1000, 2000, and 3000 rpm), three evaporator fan speeds (250, 120, and 70 cfm), and two inlet evaporator air temperatures (60 and 90°F). At each test condition, the refrigerant state into and out of the expansion valve and the refrigerant state exiting the evaporator were fully characterized using calibrated temperature and pressure transducers. Refrigerant mass flow rate was measured directly. The dry bulb and wet bulb temperatures of the air stream into and out of the evaporator were measured, along with the air flow rate.

Recall that the inlet refrigerant enthalpy, mass flow rate, and outlet pressure are required as input to the subprogram, along with the inlet air temperature, relative humidity, and air flow rate. To validate the submodel, *experimental* values for these variables were used as input; and the *calculated* capacity, sensible heat ratio, and refrigerant pressure drop were compared with the corresponding experimental results. These comparisons are shown in Fig. 8. In each of the three plots, the ordinate shows the ratio of calculated to measured values. The capacity was very well predicted for all operating conditions. The refrigerant pressure drop is well predicted at the higher values of pressure (higher flow rates) but shows greater error at the smaller flow rates. The ratio of sensible to total capacity exhibits significant scatter with a standard deviation of 24%.

4.2 SYSTEM VALIDATION

No comparison has yet been made between AHPM predictions and data obtained from a complete automobile air conditioner system. On the other hand, it is worth noting that the residential heat pump version has been well validated on a system level. Dabiri (1982), Fischer and Rice (1983), and Fischer and Rice (1985) made comparisons over wide ranges of conditions for single-speed calculations. Detailed comparisons for variable

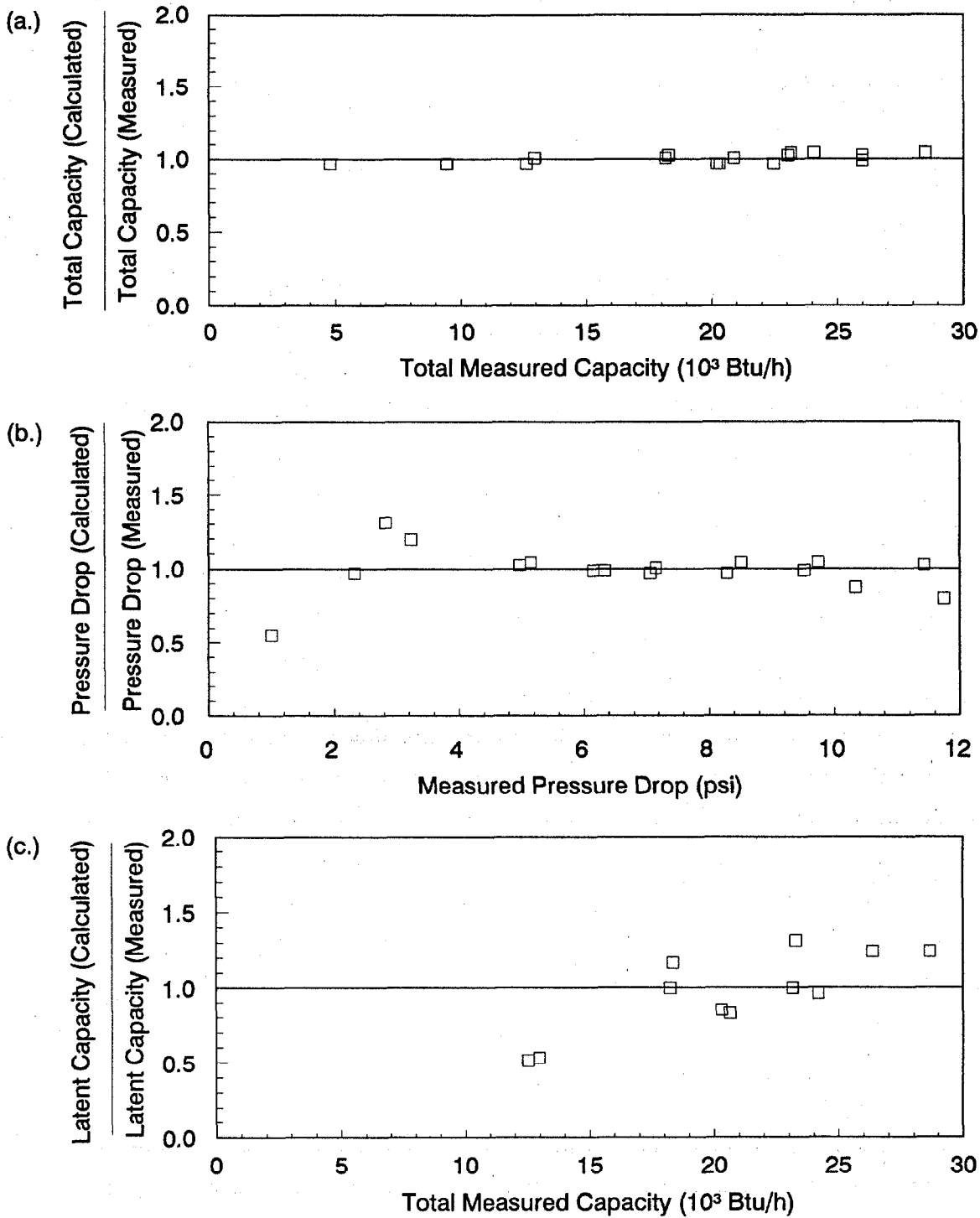


Fig. 8. Comparison of plate-fin evaporator submodel with laboratory test measurements. (a) ratio of calculated to measured capacity as a function of measured capacity. (b) Ratio of calculated to measured refrigerant pressure drop as a function of measured pressure drop. (c) Ratio of calculated capacity ratio (latent capacity divided by total capacity) to measured capacity ratio as a function of measured capacity ratio.

speed systems were carried out by Miller (1987, 1988) and by Rusk et al. (1990). Damasceno et al. (1990) compared the ORNL model with two other publicly available models, as well as with experimental data. Damasceno's results suggest that, in cases where the heat exchanger circuitry becomes complicated, significant errors in the predicted value of subcooling and/or pressure drop can occur. Yet even when such errors occur, global performance parameters such as mass flow rate, coefficient of performance (COP), and capacity are predicted to within $\pm 10\%$. For simple heat exchanger circuiting, very good accuracy has been found. Errors in specifying the compressor performance tend to result in system parameter errors of like magnitude. Thus *accurate compressor characterization is of predominant importance*. These results are expected to hold for the AHPM as well.

The first part of the document discusses the importance of maintaining accurate records of all transactions. It emphasizes that proper record-keeping is essential for the success of any business and for the protection of the interests of all parties involved. The document then goes on to describe the various methods and techniques used to collect and analyze data, highlighting the need for consistency and reliability in the information gathered.

The second part of the document focuses on the analysis of the collected data. It discusses the various statistical methods and techniques used to interpret the results, and how these can be used to identify trends and patterns in the data. The document also discusses the importance of comparing the results of the analysis with the expected outcomes, and how this can be used to evaluate the effectiveness of the program or project.

The final part of the document discusses the implications of the findings and the need for further research. It emphasizes that the results of the analysis should be used to inform decision-making and to guide the development of future programs and projects. The document also discusses the need for ongoing monitoring and evaluation to ensure that the program or project remains effective and relevant over time.

5. OVERVIEW OF PROGRAM USAGE

5.1 DESIGN/OPTIMIZATION STUDIES

The AHPM can serve as a useful tool in many different types of studies. It is instructive to group these studies into two classes: (1) design/optimization studies and (2) simulation studies. Design/optimization studies consist of using the AHPM to help specify all, or nearly all, of the *system components*, given *known operating conditions* (e.g., air temperatures) and *known system capacity* requirements. Such studies lead to component selections that best satisfy the user's design criteria; in other words, they lead to an optimal design. Two common criteria for optimization are seasonal efficiency and capital cost. It is beyond the scope of this report to explore such design strategies in detail. We note however that Rice (1992) has developed a rational methodology for designing a heat pump system having a maximum seasonal energy efficiency, using the residential heat pump version. His paper should prove informative to anyone interested in using the AHPM for design/optimization studies, regardless of the optimization criteria.

5.2 SIMULATION STUDIES

Simulation studies begin with a full, or nearly full, set of specified components. Such studies are aimed at understanding how the specified system behaves as the operating conditions are varied (e.g., air temperatures), or as one of the component parameters is varied (e.g., evaporator fin surface area, refrigerant mass, fan speed). The following procedure is offered as a guide to help obtain the most accurate simulations possible with the AHPM. The procedure assumes that the refrigerant mass is unknown. *This assumption should always be made, regardless of whether the refrigerant mass is actually known for the system being simulated.* For users who do not wish to specify the expansion device at the outset, the procedure provides a method for allowing the program to automatically calculate the expansion device size required by the system. The procedure is summarized schematically in Fig. 9.

1. Prepare the input data file (see Sect. 6) by specifying all components and system configuration options, with the following exceptions: Omit the refrigerant charge

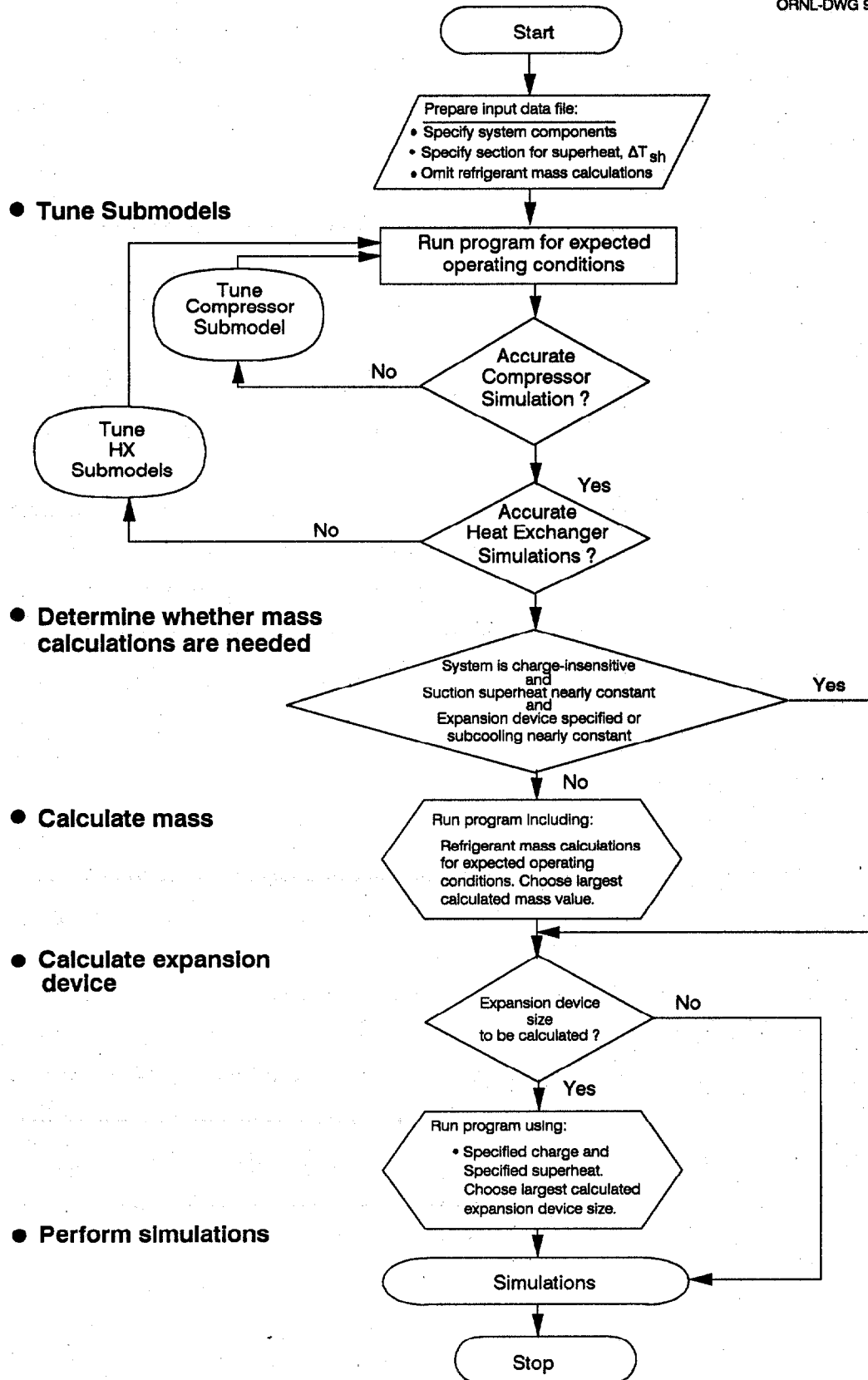


Fig. 9. Flow chart depicting recommended methodology for simulation studies using the Automobile Heat Pump Model.

calculations (see lines 4 and 5 of input data file). Recall from Sect. 3.1 that omission of the charge requires that the suction superheat be specified in its place (line 4). Also, omit the specification of the expansion device at this point, *whether it be known or not*. Recall from Sect. 3.1 that subcooling leaving the condenser must be specified in its place (line 6).

2. Run the AHPM for several different operating conditions, spanning the parameter ranges of interest, and assign a different name to the output file each time (the program always prompts for the output file name). Study the details given in the output files concerning the evaporator performance, the condenser performance, and the compressor performance. Confirm that the simulated performances are reasonable. If performance data are available, make quantitative comparisons between simulations and data.
3. Tune the compressor submodel to rectify the errors observed in the results. Tuning should be done in one of two ways, depending upon the type of error:
Systematic bias: If at some rpm setting, similar errors occur at all suction and discharge pressures, then use the mass flow adjustment factor and power adjustment factor (line 10.2 of AHPM input file).
Curve-fitting errors: If errors in simulated performance appear for only particular values of suction or discharge pressure, then the curve fits themselves may have deviated from the compressor data. Check the data being input to the curve fitting routine (see Appendix B). It may be beneficial to use the weighting factors specified in that curve-fitting input file to correct curve-fitting errors, especially in the case of sparse data.

When compressor tuning is completed, repeat step 2.

4. Tune the heat exchanger submodels to reduce the errors observed in the results. Use the heat transfer and pressure drop multipliers for the indoor coil (line 17) and for the outdoor coil (line 23). Repeat step 2.
5. This step is provided to determine the proper refrigerant mass for the system. In some cases, it may be simultaneously true that (a) the system is charge-insensitive, (b) the superheat is nearly constant, and (c) the expansion device is known or the subcooling is nearly constant. If *all three* of these conditions are true, then this step can be skipped.

Otherwise, to find the correct charge, first run the AHPM *including* the refrigerant mass calculations (line 4) for a variety of operating conditions that span the range of interest. Because the mass is being *calculated* and not *specified*, the superheat (line 4) must be specified. If the expansion device is known, it can be specified at this point. If the expansion device is to be treated as unknown, then the subcooling must again be specified (line 6). A good choice for specifying the superheat (and subcooling) values is the average value(s) expected in the actual system for the given operating range. An even better choice would be to specify various superheat (and subcooling) value(s) in accordance with performance data indicating how the values change in the actual system for the operating range. The *largest* value for the total refrigerant mass obtained from the various runs will now serve as the specified charge in subsequent calculations.

6. This step is provided for determining the proper expansion device for the system. If the expansion device has been specified already, this step can be skipped. Note that the expansion device sizing and the refrigerant charge are strongly interdependent, so that it is nonsensical to perform this step without first performing step 5. The expansion device for the charged system is easily found by choosing the control option depicted in Fig. 7b (Sect. 3). Thus the AHPM is run using a *specified refrigerant charge* calculated above in step 5 (lines 4, 5, 6) and a *specified superheat*. Recall from Sect. 3 that in this case, the only way to avoid an overdetermined system is to specify *nothing* concerning either the expansion device or the subcooling. The AHPM will in this case calculate the subcooling *and* associated expansion device dimensions required for a solution (Fig. 7b). Run the AHPM in this way for the desired range of operating conditions, noting the calculated expansion device dimensions in each case. The *largest* dimensions from all of the runs will now serve as the specified expansion device in subsequent calculations.

Note: Runs using a *specified refrigerant charge* calculated in step 5 and a *specified superheat* can also be regarded as a means of modeling a somewhat idealized TXV system. Actual cross-charged TXVs do not maintain a strictly constant superheat at the evaporator exit; variations in superheat can actually be as much as 7 or 10° F. Over a limited range of operating conditions, it often can be reasonable to approximate the system performance by fixing the superheat, letting the subcooling float (Fig. 7b). This option has the advantage of avoiding using the TXV subprogram (see Sect. 2).

7. Run the completed model for a variety of conditions. In the particular case where the TXV submodel is used, we recommend using an initial guess for the superheat (line 4) of about 1°F, to ensure the fastest convergence to a stable solution.

5.3 MODEL AVAILABILITY AND SOFTWARE REQUIREMENTS

The AHPM described in this report is available to the research community for use. The source program is written using FORTRAN 77. It is modularized so that manufacturers with proprietary components can customize the program to their needs. The program and ancillary files are distributed on one double-sided high-density diskette of 1.4 Mb capacity. An executable file for MS-DOS is available which does not require a math coprocessor, but which will use the coprocessor if it is present. To use the code with other computer operating systems, users must have their own FORTRAN compiler to create an executable file.

The author can be contacted directly regarding specifics on how copies of the model can be obtained for development and research purposes. It is hoped that the model capabilities described in this report will encourage U.S. manufacturers to obtain the program and to investigate further its use in designing high-efficiency automotive heat pumps.

...the ... of ...

...the ... of ...

...the ... of ...

...the ... of ...

...the ... of ...

6. INPUT DATA FILE

This section describes in detail the parameters required on each line of the input data file, their variable names, and their numerical formats. It is assumed that the user has carefully read Sects. 2, 3, and 5 and that he or she will refer to these while completing the input data file.

A sample input data file is seen in Fig. 10. The variable values shown in Fig. 10 are also given as sample values in the line-by-line description that follows. The sample data values represent a typical automobile air conditioning system of modern design. The structure of the input file is affected by the choice of compressor representation (variable-speed or explicit efficiency submodels) and by the choice of evaporator configuration (plate-fin or finned tube). Structural changes are shown in Fig. 8 by the use of the dashed outlined boxes that can be interchanged. *Note that this section describes only input files for systems using open compressors.* To model systems using electric-driven hermetic compressors, users are referred to documentation for the residential heat pump version by Rice (1991)

6.1 TITLE AND CONTROL DATA

Line 1	Variable	HTITLE
	Columns	1 - 80
	Format	A80
	Sample	SAMPLE

HTITLE Descriptive title for heat pump system defined by this data set.

Line 2	Variable	LPRINT
	Columns	1 - 10
	Format	I10
	Sample	1

LPRINT Output switch to control the type and amount of printed results:
=0, for minimum heat pump model output with only an energy input and output summary.
=1, for a summary of the system operating conditions and component performance calculations as well as the energy summary.
=2, for output *after* each intermediate iteration converges.
=3, for continuous output *during* intermediate iterations.

VARIABLE-SPEED AIR CONDITIONER; PLATE-FIN EVAPORATOR; 30 MPH.

1								
1	12							
0	10.0	0.0	0					
0	10.0	4.834	0.035	0.040	2.5	0.68		
0	16.0	0.0	0.0	0.0	0.0	0.0		
37.4	155.							
2	9.800	2000.	0.0	0.90				
0.0E+00	0.0E+00	0.0E+00						
TECUMSEH HR980 COMPRESSOR:								
9.8000	-65.0000							
1000.0000	1.0	1.0						
1.690E-04	-4.523E-02	2.500E-04	-2.178E-02	2.113E-04	4.182E+00			
3.463E-02	-1.274E+01	-7.500E-03	8.887E+00	-1.015E-02	1.132E+03			
2000.0000	1.0	1.0						
7.239E-05	4.990E-03	5.250E-04	4.999E-02	-1.209E-04	-3.937E-01			
3.957E-03	-3.560E+00	4.000E-02	1.128E+01	-2.171E-02	5.469E+02			
3000.0000	1.0	1.0						
-1.796E-04	9.979E-02	6.000E-04	1.530E-01	-6.193E-04	-8.402E+00			
-3.215E-02	6.782E+00	8.750E-02	1.124E+01	-2.028E-02	-1.062E+02			
4000.0000	1.0	1.0						
-3.594E-04	1.678E-01	7.500E-04	2.314E-01	-9.974E-04	-1.416E+01			
-6.521E-02	1.682E+01	1.025E-01	1.460E+01	-2.907E-02	-8.267E+02			
5000.0000	1.0	1.0						
-5.441E-04	2.381E-01	9.000E-04	3.258E-01	-1.502E-03	-2.023E+01			
-8.410E-02	2.225E+01	1.325E-01	1.599E+01	-3.220E-02	-1.179E+03			
85.0	0.52							
175.	148.	0.15						
.TRUE.								
0.52	4.33	1.8	9.250	0.70	72.0			
10.7	45.0	3.1000	14.000	0.0060	95.0	95.0		
1.167								
1.0	1.0	1.0	1.0	1.0				
95.0	0.80							
2600.	110.							
3.02	2.0	2.0	0.72	1.00	32.0			
3.00	10.	.006	0.375	0.325	95.0	95.0	999.	
3	0.092							
1.0	1.0	1.0	1.0	1.0				
0	0							
100.	100.	100.						
0.2555	39.8	0.6860	31.00	0.6860	2.00			
0.7930	5.00	0.5610	2.00					
0.05	0.05	0.40	0.10	0.0015	0.05	0.0005	0.00003	
0.70 0.05								
Explicit Efficiency Submodel								
Variable-Speed Submodel								
Plate Fin Heat Exchanger Submodel								
Finned-Tube Heat Exchanger Submode								
0.58	5.0	4.0	0.625	1.00	82.			
3.0	11.	.005	0.375	0.325	95.0	95.0	999.	
3	0.092							

Fig. 10. Sample input data file "HPDATA." Boxed data illustrate the changes in the structure of the data file that result from the choice of compressor submodel and of the indoor heat exchanger submodel.

Line 3

Variable	NCORH	NR
Columns	1 - 10	11 - 20
Format	I10	I10
Sample	1	134

NCORH Switch to specify cooling or heating mode:

=1, for cooling mode.

=2, for heating mode.

NR Refrigerant number—12, 22, 114, 502, or 134

(If NR is omitted, the default is R12).

6.2 REFRIGERANT MASS DATA

Line 4

Variable	ICHRGE	SUPER	REFCHG	MVOID
Columns	1 - 10	11 - 20	21 - 30	31 - 40
Format	I10	F10.4	F10.4	I10
Sample	0	10.0	3.0	0

ICHRGE Indicator for specifying mass balance choice:

=0, Charge is *not* specified; It is calculated as a part of the solution.

Compressor inlet superheat must be specified using SUPER.

=1, Charge is specified, along with all other major components.

Neither superheat nor subcooling can be specified.

=2, Charge is specified. Neither the expansion device nor the subcooling is specified. Compressor inlet superheat is therefore specified to avoid underdetermined system.

SUPER ≥ 0 , Compressor inlet superheat ($^{\circ}\text{F}$). If ICHARGE=0 or 2, then this is the *specified* value. If ICHARGE=1, then this is the *estimated* (fixed) value.

< 0 , Negative of the quality at the compressor inlet. Same dependence on ICHARGE as above.

REFCHG Specified system refrigerant charge (lbm); Not needed if ICHARGE=0.

MVOID Switch to specify heat exchanger void fraction (slip) method for charge inventory calculations:

=0, Default method—Zivi void fraction model with analytical solution for a *constant heat flux* approximation.

> 0 , various user-selected void fraction models with *variable heat flux* effects (which require slower numerical solutions).

Mass-flow independent methods:

=1, Homogeneous (no slip)

=2, Zivi

=3, Lockhart-Martinelli

- =4, Thom
- =5, Baroczy

Mass-flow dependent methods:

- =6, Hughmark
- =7, Premoli
- =8, Tandon

Notes: (1) For an explanation of the various void fraction models, see Rice (1987). (2) If a plate fin evaporator is selected, then the Zivi model is automatically used to calculate refrigerant mass in the evaporator. MVOID can still be used to select the calculation method used in all other system components.

Line 5

Variable	IMASS	ACCHGT	ACCDIA	OILDIA	UPPDIA	HOLDIS	ATBDIA
Columns	1 - 10	11 - 20	21 - 30	31 - 40	41 - 50	51 - 60	61 - 70
Format	I10	F10.4	F10.4	F10.4	F10.4	F10.4	F10.4
Sample	1	10.0	4.83	.0350	.040	2.5	.68

- IMASS** Switch for option to omit refrigerant charge calculations, only active if ICHARGE=0 case:
 =0, if charge calculations are to be omitted.
 =1, if charge calculations are to be made.
- ACCHGT** Height of accumulator (in.).
- ACCDIA** Internal diameter of accumulator (in.).
- OILDIA** Inner diameter of oil return hole J-tube (in.).
- UPPDIA** Inner diameter of upper hole in J-tube (in.).
- HOLDIS** Vertical distance between holes (in.).
- ATBDIA** Inner diameter of J-tube (in.).

Notes: See Fig. 11 for explanation of the accumulator geometry values. These values are not required if the refrigerant mass is not calculated or used (IMASS = 0 and ICHARGE = 0). If an accumulator is not used, set accumulator height ACCHGT to 0.0. IMASS is required.

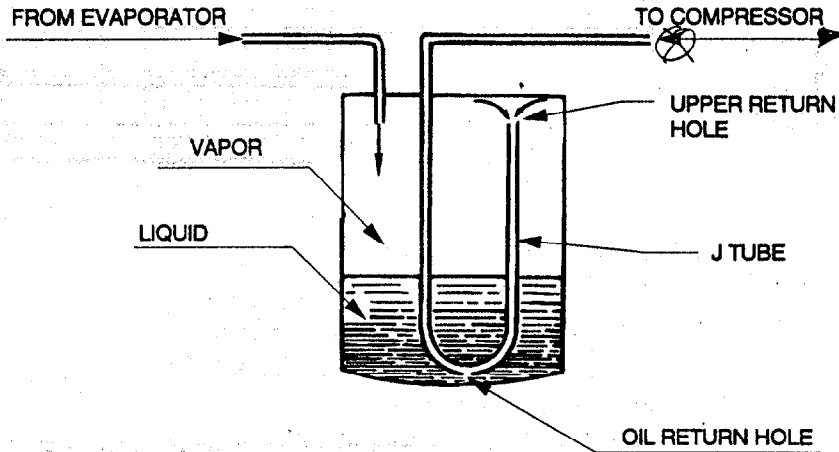


Fig. 11. Schematic of an accumulator.

6.3 EXPANSION DEVICE DATA

The number of variables given on line six and their names depend upon the choice submodel.

Expansion Device Unspecified

Line 6

Variable	IREFC	DTROC
Columns	1 - 10	11 - 20
Format	I10	F10.4
Sample	0	16.0

IREFC = 0

DTROC Refrigerant subcooling at the condenser exit ($^{\circ}$ F or negative of the desired quality for the case of incomplete condensation).

Notes: When IREFC=0, DTROC is the specified (fixed) subcooling, except if both the refrigerant charge and the superheat are specified (see description for ICHARGE = 2 in line 4; see also discussion in Sects. 3.1 and 3.2). In this latter case, DTROC serves as an initial estimate for the subcooling (see Fig. 7b).

Thermostatic Expansion Valve:

Line 6

Variable	IREFC	TXVRAT	STATIC	SUPRAT	SUPMAX	BLEEDF	NZTBOP
Columns	1 - 10	11 - 20	21 - 30	31 - 40	41 - 50	51 - 60	61 - 70
Format	I10	F10.4	F10.4	F10.4	F10.4	F10.4	F10.4
Sample	1	2.0	6.0	11.0	13.0	1.0	0.0

IREFC =1
 TXVRAT Rated capacity of the TXV (ton).
 STATIC Static superheat setting for the TXV (°F).
 SUPRAT TXV superheat at rating conditions (°F).
 SUPMAX Maximum effective operating superheat (°F).
 BLEEDF TXV bypass or bleed factor.
 NZTBOP Switch to omit TXV nozzle and tube pressure drop calculations:
 =0.0, to omit tube and nozzle pressure drops.
 =1.0, to include tube and nozzle pressure drop calculations.

Notes: See Fig. 12 for an explanation of TXV performance parameters. NZTBOP concerns the distributor nozzle and tubes that are sometimes used to equalize refrigerant flow in each evaporator circuit. These are omitted on many automobile TXVs. For a discussion of the pressure drop calculation, see Fischer and Rice 1983.

Capillary Tube:

Line 6

Variable	IREFC	CAPFLO	NCAP
Columns	1 - 10	11 - 20	21 - 30
Format	I10	F10.4	F10.4
Sample	2	3.8	1.0

IREFC =2
 CAPFLO Capillary tube flow factor, see ASHRAE Handbook, Equipment Vol. (1988), Fig. 39, p. 19.27.
 NCAP Number of capillary tubes in parallel.

Short Tube Orifice:

Line 6

Variable	IREFC	ORIFD
Columns	1 - 10	11 - 20
Format	I10	F10.4
Sample	3	0.0544

IREFC =3
 ORIFD Diameter of the short-tube orifice (in.).

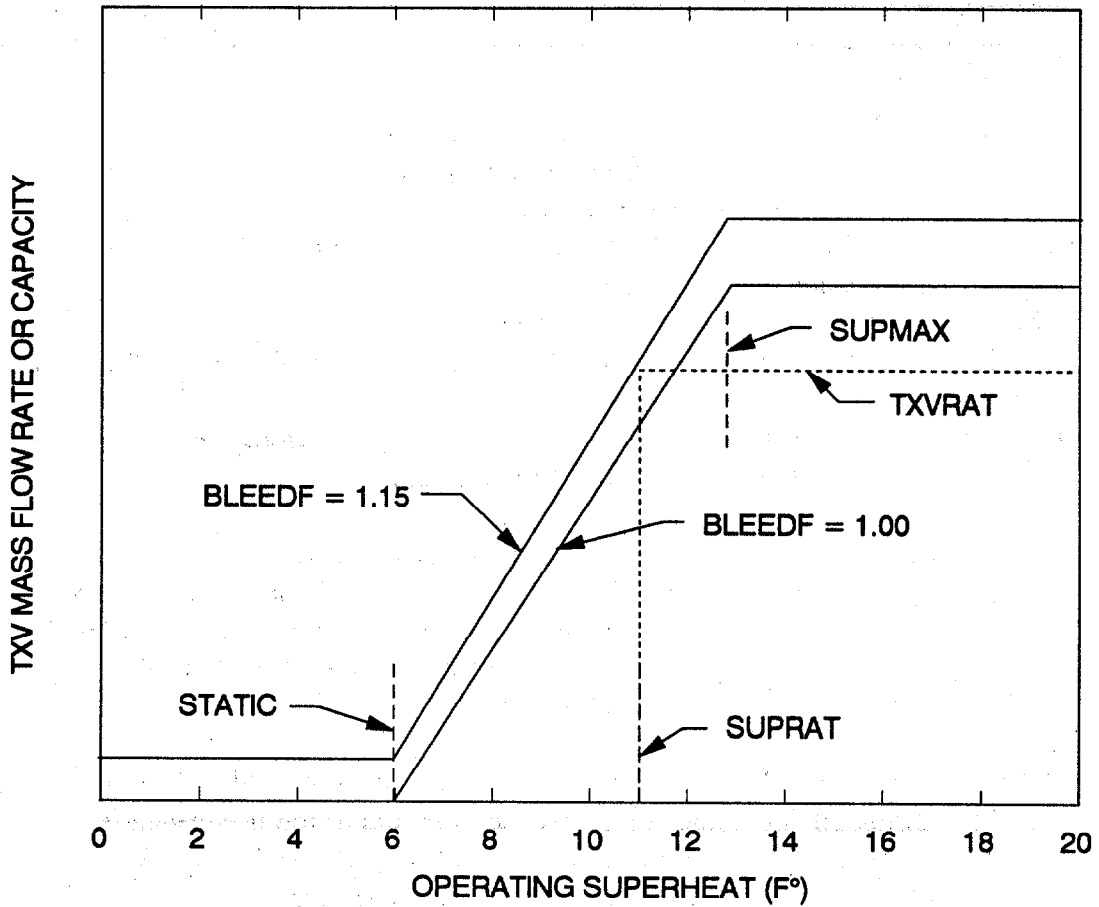


Fig. 12. Thermal expansion valve mass flow rate (or capacity). The variables shown correspond with the input variables on line 6 of the HPDATA.

6.4 COMPRESSOR DATA

Line 7

Variable	TSICMP	TSOCMP
Columns	1 - 10	11 - 20
Format	F10.4	F10.4
Sample	48.0	120.0

- TSICMP Estimate of the refrigerant saturation temperature corresponding to the pressure at compressor inlet (°F).
- TSOCMP Estimate of the refrigerant saturation temperature corresponding to the pressure at the compressor outlet (°F).

Explicit Efficiency Submodel:

Line 10.0

Variable	ETAISN	VR
Columns	1 - 10	11 - 20
Format	F10.4	F10.4
Sample	0.70	0.05

ETAISN Isentropic efficiency of the compressor:

VR Used to calculate the volumetric efficiency of the compressor.

>0, Compressor clearance volume ratio: The volumetric efficiency is calculated as a function of pressure ratio, using the clearance volume ratio, VR.

<0, Negative of the volumetric efficiency (fixed value).

Notes: For a definition of isentropic efficiency, see Eq. 1 (Sect. 2.1). The relation for calculating volumetric efficiency is described in Fischer and Rice (1983) and uses three coefficients set in BLOCK.

Variable-Speed Model:

Line 10.0

Variable	CTITLE
Columns	1 - 80
Format	A80
Sample	SAMPLE

CTITLE Descriptive title for curve-fit compressor data.

Line 10.1

Variable	NRPM	DISPLB	SUPERB
Columns	1 - 10	11 - 20	21 - 30
Format	I10	F10.4	F10.4
Sample	5	9.8	-65.000

NRPM Number of RPMs for which compressor-data curve-fits are available.

DISPLB Displacement of the compressor that is represented in the map (cubic inches).

SUPERB Superheat value for compressor map:

≥0, Base superheat entering compressor (°F).

<0, Negative of return gas temperature into compressor (°F).

Notes: Some compressor manufacturers maintain a constant return gas temperature rather than a constant suction superheat when testing their compressors.

***** Repeat lines 10.2 - 10.4 NRPM number of times *****

Line 10.2	Variable	RPMVAL	POWADJ	XMRADJ
	Columns	1 - 10	11 - 20	21 - 30
	Format	F10.4	F10.4	F10.4
	Sample	1000.00	1.0	1.0

RPMVAL Compressor speed (rpm) associated with the first set of curve-fit coefficients.

POWADJ Adjustment factor to curve-fit for power, =1.0 if value is omitted.

XMRADJ Adjustment factor to curve-fit for mass flow rate, =1.0 if omitted.

Notes: To understand how POWADJ and XMRADJ are used, see equations for lines 10.3 and 10.4. For a general discussion on when to use POWADJ and XMRADJ, see Sect. 5.2.

Line 10.3	Variable	CPOWER ₁	CPOWER ₂	CPOWER ₃	CPOWER ₄	CPOWER ₅	CPOWER ₆
	Columns	1 - 10	11 - 20	21 - 30	31 - 40	41 - 50	51 - 60
	Format	E10.3	E10.3	E10.3	E10.3	E10.3	E10.3
	Sample	1.690E-4	-4.523E-2	2.500E-4	-2.178E-2	2.113E-4	4.182E+00

CPOWER₁₋₆ Coefficients for bi-quadratic fit to *compressor power* (HP) at RPMVAL as a function of compressor suction and discharge saturation temperatures (°F), TSICMP and TSOCMP.

$$\begin{aligned} \text{POWER}(I) / \text{POWADJ} = & \text{CPOWER}_1 * \text{TSOCMP}^2 \\ & + \text{CPOWER}_2 * \text{TSOCMP} + \text{CPOWER}_3 * \text{TSICMP}^2 \\ & + \text{CPOWER}_4 * \text{TSICMP} + \text{CPOWER}_5 * \text{TSOCMP} * \text{TSICMP} \\ & + \text{CPOWER}_6 \end{aligned}$$

Line 10.4	Variable	CMASSF ₁	CMASSF ₂	CMASSF ₃	CMASSF ₄	CMASSF ₅	CMASSF ₆
	Columns	1 - 10	11 - 20	21 - 30	31 - 40	41 - 50	51 - 60
	Format	E10.3	E10.3	E10.3	E10.3	E10.3	E10.3
	Sample	3.463E-2	-1.274E+2	-7.500E-3	8.887E+00	-1.015E-2	1.132E+3

CMASSF₁₋₆ Coefficients for bi-quadratic fit to *compressor mass flow rate*, XMR (lbm/hr), at RPMVAL as a function of compressor suction and discharge saturation temperatures (°F), TSICMP and TSOCMP.

$$\begin{aligned} \text{XMR} / \text{XMRADJ} = & \text{CMASSF}_1 * \text{TSOCMP}^2 \\ & + \text{CMASSF}_2 * \text{TSOCMP} + \text{CMASSF}_3 * \text{TSICMP}^2 \\ & + \text{CMASSF}_4 * \text{TSICMP} + \text{CMASSF}_5 * \text{TSOCMP} * \text{TSICMP} \\ & + \text{CMASSF}_6 \end{aligned}$$

***** Repeat lines 10.2 - 10.4 NRPM number of times *****

6.5 INDOOR HEAT EXCHANGER DATA

Line 11

Variable	TAPII	RHII
Columns	1 - 10	11 - 20
Format	F10.4	F10.4
Sample	80.0	0.52

TAPII Air temperature entering the indoor unit (°F).

RHII Relative humidity of the air entering the indoor unit.

Line 12

Variable	QANMI	FANEFI	DDUCT
Columns	1 - 10	11 - 20	21 - 30
Format	F10.4	F10.4	F10.4
Sample	250.0	148.00	0.15

QANMI Air flow rate (cfm).

FANEFI Combined fan/fan-motor efficiency parameter:

≤ 1.0, Specified (fixed) value of combined fan/fan-motor efficiency:
Used in conjunction with QANMI and the system pressure drop
DDUCT to *calculate* the fan motor power.

> 1.0, Directly specified power (watts) of drive.

DDUCT Specified pressure drop of duct system (in. H₂O), independent of
specified air flow rate: DDUCT is not used in fan power calculations
if FANEFI > 1.0.

Notes: Electric motor power W_{mot} can be calculated either by specifying it as
fixed, or using a "first principles" approach whereby $W_{mot} =$
 $[(QANMI \times \Delta P) / FANEFI]$. In the latter case, ΔP represents the
sum of the system pressure drop DDUCT and the pressure drop
across the coil, which is calculated by the program. This option has
been included so that by varying the duct system resistance
parametrically, users may study the effect that evaporator plenum
design has on the system performance.

Line 13

Variable	PLATE
Columns	1 - 10
Format	A10
Sample	.TRUE.

PLATE Indoor Heat Exchanger Configuration:
 .TRUE. Specifies plate-fin heat exchanger.
 .FALSE. Specifies finned-tube heat exchanger.

Notes: Variables on lines 14, 15, and 16 are determined by the variable PLATE. Note that a plate-fin evaporator *can* be used with hermetic compressors ('OPEN'=.FALSE. in BLOCK.FOR).

Plate-Fin Heat Exchanger.

Line 14

Variable	AAFI	NSECTI	PLHTI	GAPAI	TPI	DEPTHI
Columns	1 - 10	11 - 20	21 - 30	31 - 40	41 - 50	51 - 60
Format	F10.4	F10.4	F10.4	F10.4	F10.4	F10.4
Sample	0.485	4.0	2.0	10.0	0.6	72.0

AAFI Frontal area of the coil (sq. ft.).
 NSECTI Number of equivalent, parallel refrigerant circuits in heat exchanger.
 PLHTI Plate height (press-molded rib height plus plate thickness, mm).
 GAPAI Gap between plates on air side (mm).
 TPI Plate thickness (mm).
 DEPTHI Length of air channels (mm).

Notes: Refer to Fig. 13 for a depiction of each variable. Note that the variable NSECTI denotes the number of adjacent refrigerant passages having flow in the same direction. Thus although there are 12 refrigerant layers and 12 air layers making up the cross-flow plate-fin heat exchanger seen in Fig. 12b, flow is parallel in only four adjacent layers before it is reversed. In this case it is correct to specify NSECTI=4.0. This subprogram, which can *only model single-pass heat exchangers*, treats the configuration in Fig. 12b as the "unfolded" single-pass configuration in Fig. 12c having four equivalent circuits. Finally, note that if there were 5 parallel circuits in the last of the three passes in Fig. 10b, and four in the top and middle passes, the correct value for NSECTI would be the *average number of adjacent parallel circuits per pass*, or $13/3 = 4.33 = \text{NSECTI}$.

Line 15

Variable	PITCHI	ANGLEI	RIBWI	FPI	DELTAI	XKPI	XKFI
Columns	1 - 10	11 - 20	21 - 30	31 - 40	41 - 50	51 - 60	61 - 70
Format	F10.4	F10.4	F10.4	F10.4	F10.4	F10.4	F10.4
Sample	10.7	45.	3.1	14.0	.006	95.0	95.0

PITCHI Distance between ribs measured perpendicular to bulk refrigerant flow (mm).
 ANGLEI Rib angled relative to bulk refrigerant flow (degrees).
 RIBWI Rib width (mm).

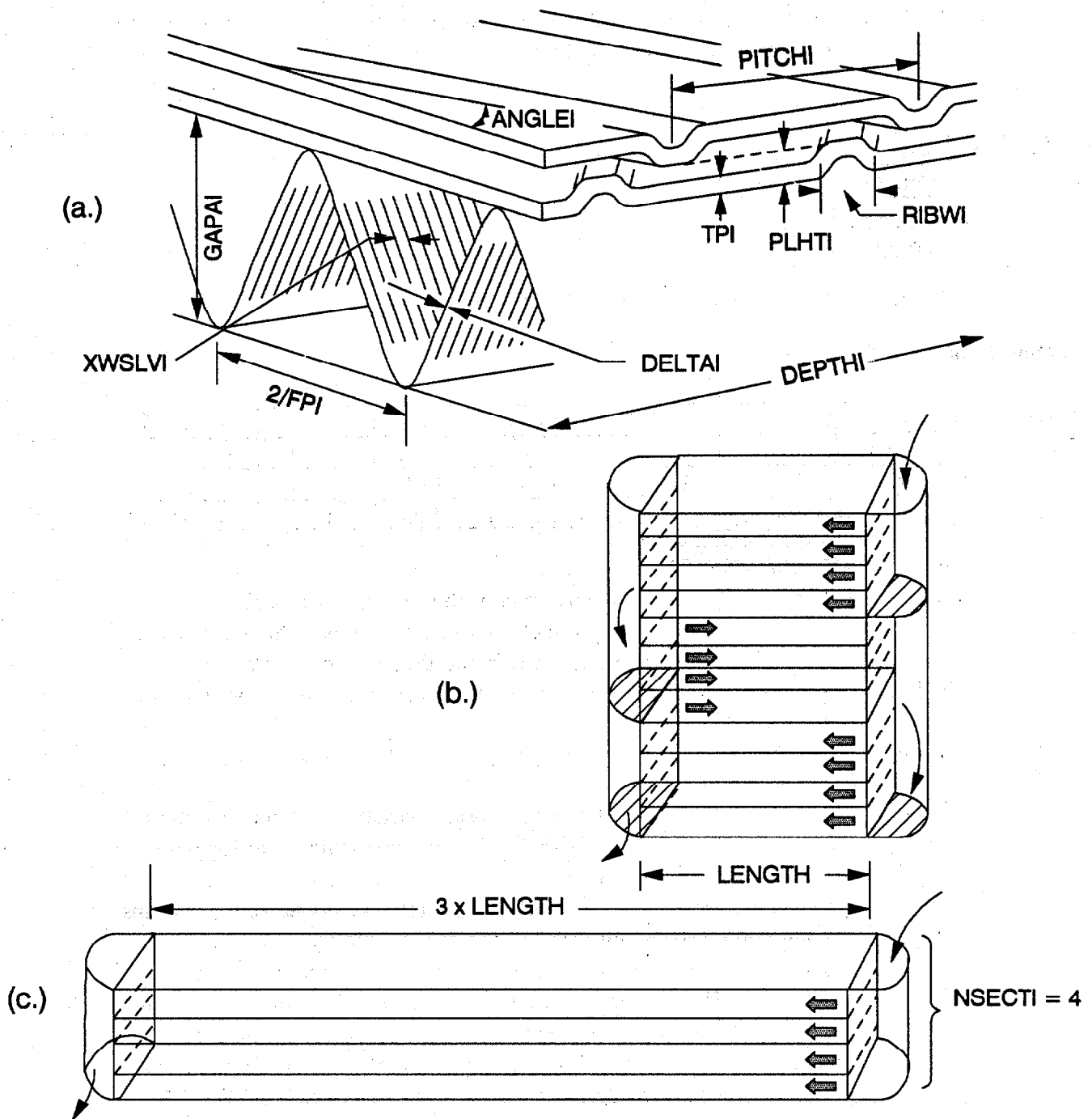


Fig. 13. Plate fin geometry.

(a) Pictorial representation of each geometric variable in lines 14, 15, and 16 in HPDATA.

(b) Example of the refrigerant circuiting in a plate-fin evaporator.

(c) Illustration of how the heat exchanger geometry shown in (b) is treated by the computer program. The three tiers in (b) are "unfolded" to make a single-tier heat exchanger with NSECTI refrigerant passages. See notes for Line 13.

- FPI Fin pitch (fins/in.).
 DELTAI Fin thickness (in.).
 XKPI Thermal conductivity of plates (Btu(hr·ft·F)⁻¹.
 XKFI Thermal conductivity of the fins (Btu(h·ft·F)⁻¹.

Line 16

Variable	XWSLVI
Columns	1 - 10
Format	F10.4
Sample	1.167

XWSLVI Width of single strip in flow direction (mm).

Finned Tube Heat Exchanger.

Line 14

Variable	AAFI	NTI	NSECTI	WTI	STI	RTBI
Columns	1 - 10	11 - 20	21 - 30	31 - 40	41 - 50	51 - 60
Format	F10.4	F10.4	F10.4	F10.4	F10.4	F10.4
Sample	0.485	2.0	1.0	0.866	1.00	68.0

- AAFI Frontal area of the coil (sq. ft.).
 NTI Number of refrigerant tube rows in the direction of air flow.
 NSECTI Number of equivalent, parallel refrigerant circuits in heat exchanger.
 WTI Spacing of the refrigerant tubes in the direction of air flow (in.).
 STI Spacing of the refrigerant tube passes perpendicular to the direction of air flow (in.).
 RTBI Total number of return bends in heat exchanger (all circuits).

Notes: Refer to Fig. 14 for a depiction of each variable. For finned-tube heat exchangers, the variable NSECTI is used differently than for plate-fin heat exchangers. For finned-tube designs, the number of equivalent circuits is simply the number of refrigerant tubes penetrating the fins in which the refrigerant starts at the initial state for the overall heat exchanger, and exits at the final refrigerant state for the overall heat exchanger. Thus in Fig. 11a, there are four parallel circuits, while in Fig. 11b, there are two. If parallel circuits are not equivalent (equal pressure drop for equal flow rate), a standard pipe circuiting analysis can be used to derive the best non-integer value for NSECTI. We give the results for the cases where there are two parallel circuits of length L_1 and L_2 :

$$N^3 = \left[1 + \frac{L_2}{L_1} \right] \left[1 + \sqrt{\frac{L_1}{L_2}} \right]^2 \quad (5)$$

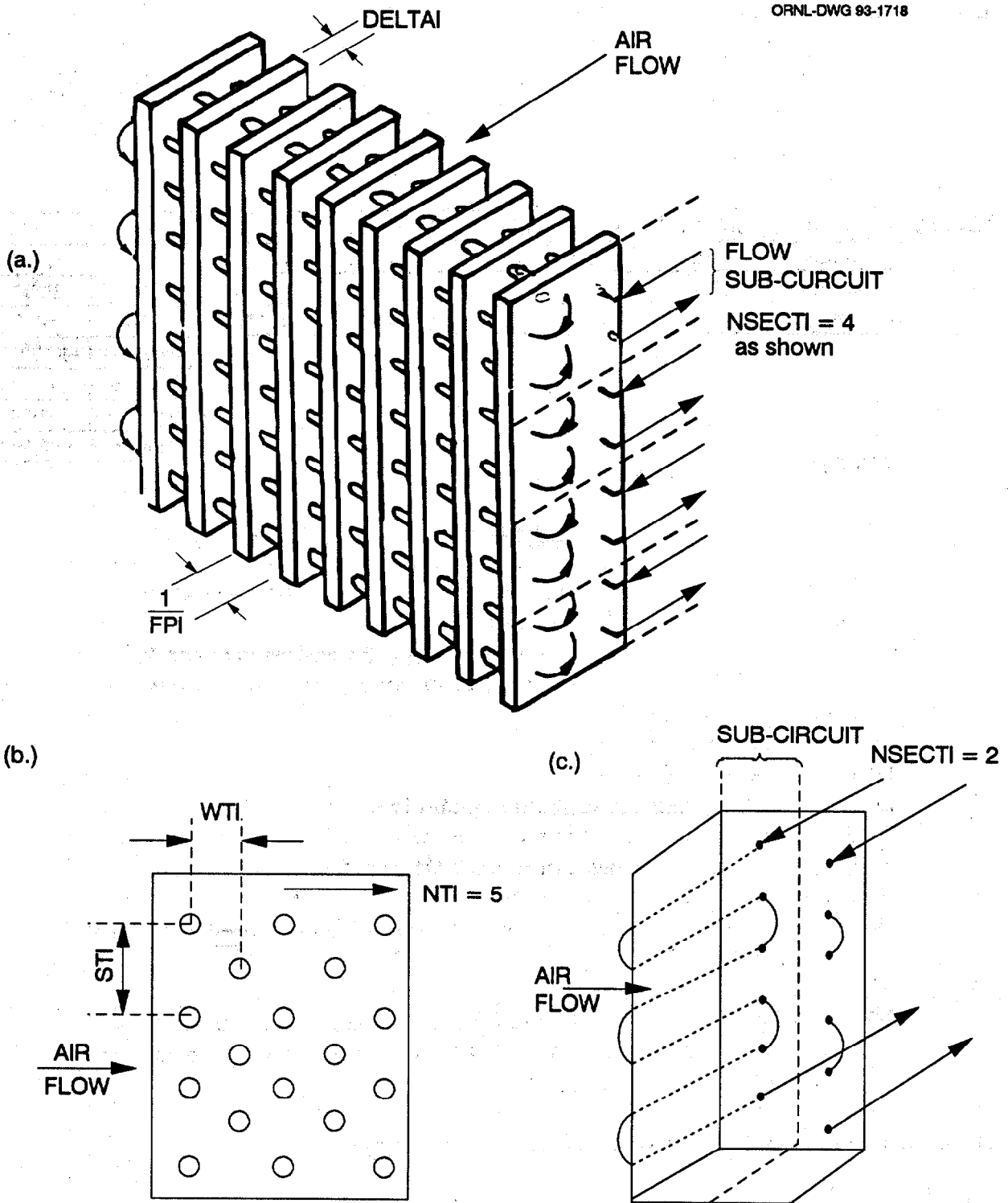


Fig. 14. Schematic drawings of finned-tube heat exchangers.
 (a) Shows the air flow geometry. Also shows refrigerant circuits.
 (b) Shows geometric variables related to staggered tube arrangement.
 (c) Shows a refrigerant circuitry arrangement that is common for automobile condensers.

and for three parallel circuits of length L_1 , L_2 and L_3 :

$$N^3 = \left[1 + \frac{L_2}{L_1} + \frac{L_3}{L_1} \right] \left[1 + \sqrt{\frac{L_1}{L_2}} + \sqrt{\frac{L_1}{L_3}} \right]^2 \quad (6)$$

Line 15

Variable	FINTYI	FPI	DELTAI	DEAI	DERI	XKFI	XKTI
Columns	1 - 10	11 - 20	21 - 30	31 - 40	41 - 50	51 - 60	61 - 70
Format	F10.4	F10.4	F10.4	F10.4	F10.4	F10.4	F10.4
Sample	3.0	14.0	0.005	0.395	0.371	95.0	95.0
						Variable	HCONTI
						Columns	71 - 80
						Format	F10.4
						Sample	999.999

FINTYI Switch to specify the type of fin surface:

=1.0 for smooth fins.

=2.0 for *general* wavy (sinusoidal) or zigzag (corrugated) fins using constant multipliers to smooth fin equations.

=3.0 for *general* louvered (simple-strip) fins using constant multipliers to smooth fin equations.

=4.0 for detailed, user-specified zigzag fin designs (see line 16).

=5.0 for detailed, user-specified louvered (simple-strip) fin designs (see line 16).

FPI Fin pitch (fins/in.).

DELTAI Fin thickness (in.)

DEAI Outside diameter of the refrigerant tubes (in.).

DERI Inside diameter of the refrigerant tubes (in.).

XKFI Thermal conductivity of the fins $(\text{Btu}(\text{hr} \cdot \text{ft} \cdot \text{F})^{-1})$.

XKTI Thermal conductivity of the tubes $(\text{Btu}(\text{hr} \cdot \text{ft} \cdot \text{F})^{-1})$.

HCONTI Fraction of the default computed contact conductance between the fins and tubes.

Notes: FINTYI and HCONTI are further documented in Rice (1991) and Fischer, Rice, and Jackson (1988) respectively. We recommend that HCONTI be kept large.

The variables given on line 16 depend upon the choice fin pattern.

FINTYI = 1,2 or 3

Line 16. Leave a blank line.

FINTYI = 4.0: Specified zigzag pattern

Line 16

Variable	NFPZGI	FPDZGI
Columns	1 - 10	11 - 20
Format	I10	F10.4
Sample	2	0.045

NFPZGI Number of fin patterns per row of tubes in flow direction.

FPDZGI Fin pattern depth (in).

FINTYI = 5.0: specified louvered pattern

Line 16

Variable	NLSVI	XLSVI	XWSLVI
Columns	1 - 10	11 - 20	21 - 30
Format	I10	F10.4	F10.4
Sample	4	8.0	2.0

NLSVI Number of strips in an enhanced zone (integer).

XLSLVI Length of enhanced louvered zone (mm).

XWSLVI Width of single strip in flow direction (mm).

Line 17

Variable	HTRMLI	PDRMLI	HTAMLI	PDAMLI	CABMLI
Columns	1 - 10	11 - 20	21 - 30		
Format	F10.4	F10.4	F10.4	F10.4	F10.4
Sample	1.0	1.0	1.0	1.0	1.0

HTRMLI Refrigerant-side heat transfer multiplier.

PDRMLI Refrigerant-side pressure-drop multiplier.

HTAMLI Air-side heat transfer multiplier.

PDAMLI Air-side *coil* pressure-drop multiplier.

CABMLI Air-side *system* pressure-drop multiplier.

Notes: For a discussion on how these multipliers are used, see Sect. 5.2.

6.6 OUTDOOR UNIT DATA

Line 18

Variable	TAIO	RHIO
Columns	1 - 10	11 - 20
Format	F10.4	F10.4
Sample	95.0	0.40

TAIO Air temperature entering the outdoor unit (°F).

RHIO Relative humidity of the air entering the outdoor unit.

Line 19

Variable	QANMO	FANEFO
Columns	1 - 10	11 - 20
Format	F10.4	F10.4
Sample	900.0	110.0

QANMO Air flow rate (cfm).
 FANEFO Directly specified power (watts) of drive.

Notes: Fan power W_{fan} must be specified directly for the outdoor fan. If its power is not considered a part of the system COP calculation, FANEFO = 0.0.

Line 20

Variable	AAFO	NTO	NSECTO	WTO	STO	RTBO
Columns	1 - 10	11 - 20	21 - 30	31 - 40	41 - 50	51 - 60
Format	F10.4	F10.4	F10.4	F10.4	F10.4	F10.4
Sample	0.485	2.0	1.0	0.866	1.00	68.0

AAFO Frontal area of the coil (sq. ft.).
 NTO Number of refrigerant tube rows in the direction of air flow.
 NSECTO Number of equivalent, parallel refrigerant circuits in heat exchanger.
 WTO Spacing of the refrigerant tubes in the direction of air flow (in.).
 STO Spacing of the refrigerant tube passes perpendicular to the direction of air flow (in.).
 RTBO Total number of return bends in heat exchanger (all circuits).

Notes: See notes for line 14 above.

Line 21

Variable	FINTYO	FPO	DELTAO	DEAO	DERO	XKFO	XKTO
Columns	1 - 10	11 - 20	21 - 30	31 - 40	41 - 50	51 - 60	61 - 70
Format	F10.4	F10.4	F10.4	F10.4	F10.4	F10.4	F10.4
Sample	3.0	14.0	0.005	0.395	0.371	95.0	95.0
						Variable	HCONTO
						Columns	71 - 80
						Format	F10.4
						Sample	999.999

FINTYO Switch to specify the type of fin surface:
 =1.0 for smooth fins
 =2.0 for *general* wavy (sinusoidal) or zigzag (corrugated) fins using constant multipliers to smooth fin equations
 =3.0 for *general* louvered (simple-strip) fins using constant multipliers to smooth fin equations
 =4.0 for detailed, user-specified zigzag fin designs (see line 16).

=5.0 for detailed, user-specified louvered (simple-strip) fin designs (see line 16).

FPO Fin pitch (fins/in.).
 DELTAO Fin thickness (in.).
 DEAO Outside diameter of the refrigerant tubes (in.).
 DERO Inside diameter of the refrigerant tubes (in.).
 XKFO Thermal conductivity of the fins (Btu(hr·ft·F)⁻¹).
 XKFO Thermal conductivity of the tubes (Btu(hr·ft·F)⁻¹).
 HCONTO Fraction of the default computed contact conductance between the fins and tubes.

Notes: FINTYO and HCONTO are further documented in Rice (1991) and Fischer, Rice, and Jackson (1988) respectively. We recommend that HCONTO be kept large.

The variables given on line 22 depend upon the choice of fin pattern.

FINTYO = 1, 2 or 3

Line 22 Leave a blank line.

FINTYO = 4.0: specified zigzag pattern

Line 22

Variable	NFPZGO	FPDZGO
Columns	1 - 10	11 - 20
Format	I10	F10.4
Sample	2	0.045

NFPZGO Number of fin patterns per row of tubes in flow direction.
 FPDZGO Fin pattern depth (in).

FINTYO = 5.0: specified louvered pattern

Line 22

Variable	NLSVO	XLSVO	XWSLVO
Columns	1 - 10	11 - 20	21 - 30
Format	I10	F10.4	F10.4
Sample	4	8.0	2.0

NLSVO Number of strips in an enhanced zone (integer).
 XLSLVO Length of enhanced louvered zone (mm).
 XWSLVO Width of single strip in flow direction (mm).

Line 23

Variable	HTRMLO	PDRMLO	HTAMLO	PDAMLO	CABMLO
Columns	1 - 10	11 - 20	21 - 30		
Format	F10.4	F10.4	F10.4	F10.4	F10.4
Sample	1.0	1.0	1.0	1.0	1.0

HTRMLO Refrigerant-side heat transfer multiplier.
 PDRMLO Refrigerant-side pressure-drop multiplier.
 HTAMLO Air-side heat transfer multiplier.
 PDAMLO Air-side *coil* pressure-drop multiplier.
 CABMLO Air-side *system* pressure-drop multiplier.

Notes: For a discussion on how these multipliers are used, see Sect. 5.2.

Line 24

Variable	MFANIN	MFANOU
Columns	1 - 10	11 - 20
Format	I10	I10
Sample	2	2

MFANIN Switch for adding heat loss from the *indoor fan* to air stream; settings are similar to those for MCMPOP.
 MFANOU Switch for adding heat loss from the *outdoor fan* to air stream; settings are similar to those for MCMPOP.

6.7 REFRIGERANT LINES DATA

Line 25

Variable	QSUCLN	QDISLN	QLIQLN
Columns	1 - 10	11 - 20	21 - 30
Format	F10.4	F10.4	F10.4
Sample	100.0	700.0	700.

QSUCLN >0, rate of heat gain in the compressor suction line (Btu/h).
 QSUCLN <0, the negative of the desired temperature rise in the suction line (°F).
 QDISLN Rate of heat loss in the compressor discharge line (Btu/h).
 QLIQLN Rate of heat loss in the liquid line (Btu/h).

Line 26

Variable	DLL	XLEQLL	DLRVIC	XLRVIC	DLRVOC	XLRVOC
Columns	1 - 10	11 - 20	21 - 30	31 - 40	41 - 50	51 - 60
Format	F10.4	F10.4	F10.4	F10.4	F10.4	F10.4
Sample	.255	39.8	.686	31.0	.686	2.0

DLL Inside diameter of the liquid line (in.).
 XLEQLL Equivalent length of the liquid line (ft.).

- DLRVIC Inside diameter of the vapor line between the reversing valve and the indoor coil (in.).
- XLRVIC Equivalent length of the vapor line between the reversing valve and the indoor coil (ft.).
- DLRVOC Inside diameter of the vapor line between the reversing valve and the outdoor coil (in.).
- XLRVOC Equivalent length of the vapor line between the reversing valve and the outdoor coil (ft.).

Line 27

Variable	DSL RV	XLEQLP	DDL RV	XLEQHP
Columns	1 - 10	11 - 20	21 - 30	31 - 40
Format	F10.4	F10.4	F10.4	F10.4
Sample	.793	0.0	.561	0.0

- DSL RV Inside diameter of the suction line from the reversing valve to the compressor inlet (in.).
- XLEQLP Equivalent length of the low-pressure line from the reversing valve to the compressor inlet (ft.).
- DDL RV Inside diameter of the discharge line from the compressor outlet to the reversing valve (in.).
- XLEQHP Equivalent length of the high-pressure line from the compressor outlet to the reversing valve (ft.).

Notes: The pressure drop through the reversing valve is not modeled. For a discussion on the effects of this omission, see Sect. 2.7. For air conditioning systems without reversing valves, the equivalent suction line length is just XLRVIC (line 26) + XLEQLP (line 27). Indeed, its entire length could be assigned to one of these variables, say XLRVIC, while the other variable =0.0. Similar remarks apply for the discharge line in an air conditioning system. Do *not* assign zero to any of the diameters in lines 26 and 27.

Line 28

Variable	EPR	PMIN	PRAT	ARAT	CVALVE
Columns	1 - 10	11 - 20	21 - 30	31 - 40	41 - 50
Format	LOGICAL	F10.4	F10.4	F10.4	F10.4
Sample	.TRUE.	44.2	200.0	0.50	

- EPR Evaporator pressure regulator (EPR): .TRUE. indicates EPS is installed. .FALSE. indicates EPS is not installed.
- PMIN Inlet pressure at which the valve allows refrigerant to pass (psia).
- PRAT Inlet pressure above which the flow area no longer increases with increasing inlet pressure.

ARAT Refrigerant flow area where inlet pressure = PRAT.
 CVALVE Valve constant.

Notes: For a definition of each operational parameter in Line 28, see Eq. 4 and Fig. 5.

6.8 SOLUTION CONVERGENCE CRITERIA

Line 29

Variable	AMBCON	CNDCON	FLOCON	EVPCON	CONMST	CMPCON	TOLH
Columns	1 - 10	11 - 20	21 - 30	31 - 40	41 - 50	51 - 60	61 - 70
Format	F10.4	F10.4	F10.4	F10.4	F10.4	F10.4	F10.4
Sample	0.2	0.2	0.2	0.50	0.003	0.05	0.001
						Variable	TOLS
						Columns	71 - 80
						Format	F10.4
						Sample	0.00005

AMBCON Convergence parameter for the iteration on evaporator inlet air temperature ($^{\circ}$ F).

CNDCON Convergence parameter for the iteration on condenser exit subcooling (or on exit quality * 200) — used when IREFC = 0 on Line 6 (F°); also the quantity $\{2 * CNDCON\}$ is used as the convergence parameter for the charge balancing iteration when ICHARGE = 2.

FLOCON Convergence parameter for iteration on refrigerant mass flow rate—used when IREFC > 0 on Line 6 (equivalent F°), value is specified as if it were in degrees F and is scaled internally (by $1/20^{th}$) to give a mass flow convergence factor.

EVPCON Convergence parameter for iteration on evaporator exit superheat (F°), (or on exit quality * 500); Also the quantity $\{2 * EVPCON\}$ is used as the convergence parameter for the charge balancing iteration when ICHARGE = 1.

CONMST Convergence parameter for iterations on evaporator tube wall temperatures in subroutine EVAP and dew-point temperature in subroutine XMOIST (F°).

CMPCON Convergence parameter for iteration on suction gas enthalpy in the efficiency-and-loss compressor model (Btu/lbm)—used only when ICOMP = 1 on Line 8.

TOLH Tolerance parameter used by refrigerant routines in calculating properties of superheated vapor when converging on a known *enthalpy* value (Btu/lbm).

TOLS

Tolerance parameter used by refrigerant routines in calculating properties of superheated vapor when converging on a known *entropy* value (Btu/lbm/°R).

7. SUMMARY

A numerical tool for simulating the operation of automobile air conditioners has been developed. The model is intended both for use as a *design and optimization* tool, and for use in *simulating* how a system will behave with *specified* components. The variable speed compressor model accommodates any positive displacement compressor whose performance can be represented as a function of suction and discharge pressures and shaft speed. Variable speed studies generally require a refrigerant mass capability, as redistribution of refrigerant for off-design conditions can affect performance significantly. Refrigerant charge distribution can be evaluated with any configuration available with this model.

Most components found in automobile air conditioning systems are represented in the code. An important exception is the condenser submodel, which handles only round, fin-and-tube configurations. All of the submodels in the residential version have been preserved in the AHPM, enabling the design and optimization of electrically powered systems. System validation remains incomplete; however, the most extensive new submodel, the plate-fin evaporator, has been shown to exhibit good accuracy when compared with laboratory data over a wide range of system operating conditions.

Memorandum

Reference is made to the report of the Committee on the Administration of the Government, dated 1954, and to the report of the Committee on the Organization of the Government, dated 1955. The Committee on the Administration of the Government has recommended that the Government should be reorganized so as to be more efficient and economical. The Committee on the Organization of the Government has recommended that the Government should be reorganized so as to be more efficient and economical.

The Government has decided to accept the recommendations of the Committee on the Administration of the Government and the Committee on the Organization of the Government. The Government has decided to accept the recommendations of the Committee on the Administration of the Government and the Committee on the Organization of the Government.

REFERENCES

- ASHRAE (American Society of Heating, Refrigerating, and Air-Conditioning Engineers, Inc.) 1988. *ASHRAE Handbook—1988 Equipment*, Atlanta.
- Beecher, D. T., and T. J. Fagan 1987. "The Effects of Fin Pattern on Air-Side Heat Transfer Coefficients in Plate Finned-Tube Heat Exchangers," *ASHRAE Transactions* 93 (Pt. 2).
- Cohen, M., and V. P. Carey 1989. "A Comparison of the Flow Boiling Performance Characteristics of Partially-Heated Cross-Ribbed Channels with Different Rib Geometries," *Int. J. Heat Mass Transfer* 32(12), 2459-74.
- Dabiri, A. E. 1982. "A Steady-State Computer Simulation Model for Air-to-Air Heat Pumps," *ASHRAE Transactions* 88 (Pt. 2), 973-87.
- Damasceno, G. S., V. W. Goldschmidt, and S. P. Rooke 1990. "Comparison of Three Steady-State Heat Pump Computer Models," *ASHRAE Transactions* 96 (Pt. 2), 191-204.
- Damasceno, G. S., S. P. Rooke, and V. W. Goldschmidt 1991. "Effects of Reversing Valves on Heat Pump Performance," *International Journal of Refrigeration* 14 (March), 93-7.
- Davenport, C. J. 1981. "Heat Transfer and Flow Friction Characteristics of Louvered Heat Exchanger Surfaces," in *Heat Exchangers: Theory and Practice*, ed. J. Taborek, G.F. Hewitt, and N. Afgan, Hemisphere Publishing, New York.
- Dieckmann, J. June 1992. "Variable Speed Compressor, HFC-134a Based Air Conditioning System," presented at the Session on Climate Control for Vehicles, ASHRAE Annual Meeting, Baltimore.
- Domanski P., and D. Didion May 1983. *Computer Modeling of the Vapor Compression Cycle with Constant Flow Area Expansion Device*, NBS Building Science Series 155, National Bureau of Standards, Gaithersburg, Md.
- Ellison, R. D., and F. A. Creswick 1978. *A Computer Simulation of Steady State Performance of Air-to-Air Heat Pumps*, ORNL/CON-16, Oak Ridge National Laboratory.
- Fadel, G. M. 1988. *Simulation of Domestic Heat Pumps with Non-Azeotropic Working Fluids and Impact of Parallel Computers on the Simulation of Thermal Systems*, Ph.D. dissertation, Georgia Institute of Technology, Atlanta.
- Fischer, S. K., and C. K. Rice 1983. *The Oak Ridge Heat Pump Models: I. A Steady-State Computer Design Model of Air-to-Air Heat Pumps*, ORNL/CON-80/R1, Oak Ridge National Laboratory, August.
- Fischer, S. K., C. K. Rice, and W. L. Jackson 1988. *The Oak Ridge Heat Pump Model: Mark III Version Program Documentation*, ORNL/TM-10192, Oak Ridge National Laboratory, March.

- Hill, J. M., and S. M. Jeter 1991. "An Enhanced Model for a Variable Speed Air Conditioner," *AES* 24, 79-84, American Society of Mechanical Engineers, New York.
- Hiller, C. C., and L. R. Glicksman 1976. "Improving Heat Pump Performance via Compressor Capacity Control—Analysis and Test, Vols. I and II," Massachusetts Institute of Technology Energy Laboratory Report MIT-EL 76-001, Cambridge, Mass.
- Kandlikar, S. G. 1991. "A Model for Correlating Flow Boiling Heat Transfer in Augmented Tubes and Compact Evaporators," *J. of Heat Trans.* 113, 966-72.
- Kays, W. M., and A. L. London 1974. *Compact Heat Exchangers*, McGraw-Hill Book Company, New York.
- Krishnan, R. R. 1986. "Evaluating Reversing Valve Performance in Heat Pump Systems," *ASHRAE Transactions*, 92 (Pt.2), 71-80.
- Lovich, M. A., and V. P. Carey 1990. "Assessment of the Combined Pressure Drop and Heat Transfer Performance of a Cross-Ribbed Channel Geometry in a Compact Evaporator Cold Plate," *Intl. Heat Transfer Conf.* 5, 27-32.
- McElgin, J., and D. C. Wiley March 1940. "Calculation of Coil Surface Areas for Air Cooling and Dehumidification," in *Heating Piping and Air Conditioning*, pp. 195-201.
- Mei, V. C. 1982. "Short-Tube Refrigerant Flow Restrictors," *ASHRAE Transactions* 88 (Pt. 2), 157-68.
- Miller, W. A. 1987. "Steady-State Refrigerant Flow and Airflow Control Experiments Conducted on a Continuously Variable Speed Air-to-Air Heat Pump," *ASHRAE Transactions* 93 (Pt. 2), 1191-1204.
- Miller, W. A. April 1988. "Laboratory Capacity Modulation Experiments, Analyses, and Validation," pp. 7-21 in *Proceedings of the 2nd DOE/ORNL Heat Pump Conference: Research and Development on Heat Pumps for Space Conditioning Applications*, CONF-8804100, Washington, D.C.
- Rice, C. K. 1987. "The Effect of Void Fraction Correlation and Heat Flux Assumption On Refrigerant Charge Inventory Predictions," *ASHRAE Transactions*, 93 (Pt. 1), 341-67.
- Rice, C. K. April 1988. "Capacity Modulation Component Characterization and Design Tool Development," pp. 22-3 in *Proceedings of the 2nd DOE/ORNL Heat Pump Conference: Research and Development on Heat Pumps for space Conditioning Applications*, CONF-8804100, Washington, D.C.
- Rice, C. K. 1991. *The ORNL Modulating Heat Pump Design Tool—User's Guide*, ORNL/CON-343, Oak Ridge National Laboratory.
- Rice, C. K. 1992. "Benchmark Performance Analysis of an ECM-Modulated Air-to-Air Heat Pump with a Reciprocating Compressor," *ASHRAE Transactions*, 98 (Pt. 1), 430-50.

Rice, C. K., and S. K. Fischer 1985. "A Comparative Analysis of Single- and Continuously Variable-Capacity Heat Pump Concepts," pp. 57-65 in *Proceedings of the DOE/ORNL Heat Pump Conference: Research and Development on Heat Pumps for Space Conditioning Applications*, Washington, D.C., December 11-13, 1984, CONF-841231.

Rusk, R. P., J. H. Van Gerpen, R. M. Nelson, and M. B. Pate 1990, "Development and Use of a Mathematical Model of an Engine-Driven Heat Pump," *ASHRAE Transactions* 96 (Pt. 2), 282-90.

Wijaya, H. 1991. "An Experimental Evaluation of Adiabatic Capillary Tube Performance for HFC-134a and CFC-12," pp. 474-83 in *Proceedings of the International CFC and Halon Alternative Conference, December 3-5*, Baltimore.

Handwritten text, likely a header or introductory paragraph, containing several lines of cursive script.

Second line of handwritten text, continuing the narrative or list.

Third line of handwritten text, possibly a concluding sentence or a separate entry.

Appendix A
DESCRIPTION OF SUBROUTINE CHANGES

A.1 OVERVIEW OF OPEN COMPRESSOR CAPABILITY: "OPEN"=.TRUE

This section briefly describes the changes that have been made to the FORTRAN subroutines in the residential model in order to compose the AHPM. The new commands themselves can be quickly found in each of the subroutines listed below by searching for the logical variables "OPEN" and "PLATE." New commands always follow an "IF (OPEN) THEN" or "IF (PLATE) THEN" logical IF statement. If both "OPEN" and "PLATE" are "FALSE," then the program behaves exactly like the residential version.

Map-Based Compressor Submodel (CMPMAP)

Most of the changes in CMPMAP are related to the fact that the independent variable used to define the *speed* of an electric hermetic compressor is the frequency of the alternating current delivered to the compressor. In the residential version, the compressor performance at any frequency can usually be found by simple interpolation between the curve-fits obtained for discrete frequencies. If the user wishes to examine alternate motors or motor sizes however, then correlations interrelating the "slip" of the motor, its efficiency, its torque, and the efficiency of the electronic frequency modulator must be evaluated.

Automobile compressor manufacturers measure actual shaft power and m at each rpm for belt-driven open compressors. As a result, the body of code that is involved with interdependence of electrical parameters could be eliminated from the automobile version. Power and m are always calculated at the desired rpm by interpolation between fits for discrete rpms.

Manufacturers' performance data do not indicate the amount of heat that is released from the compressor body. This is necessary to determine the temperature of the exiting refrigerant. The algorithm for calculating the heat loss of "thermal efficiency" has been completely changed. In the residential version, the user must specify the heat released from the hermetic shell, either as a constant or as a function of discharge temperature. Thermal efficiency is then calculated internally. It is thought that engineers dealing with open, automobile compressors are more likely to have quantitative information concerning the efficiency than concerning the rate of heat loss. For this reason, the user of the AHPM will specify the thermal efficiency, either as a constant or as a function of discharge temperature. The heat released will then be calculated as a percentage of the power, once the power is known. Other changes to CMPMAP include declaration statements, common blocks, and WRITE statements that have been changed in accordance with these modifications.

Explicit Efficiency Compressor Submodel (COMP)

In the explicit efficiency submodel of the residential version of the heat pump model, the user specifies an "internal" isentropic efficiency, which applies between the suction and discharge valve ports of the actual compressor inside of the hermetic shell. Given the enthalpy at the suction port, the enthalpy at the discharge port is then known. The enthalpy at the entrance to the shell is equal to the enthalpy at the suction valve port *plus* the heat gained in the suction line connecting the two. Similarly, between the discharge port and the shell exit, heat conducts across the discharge tube wall. These conduction rates depend upon the temperature of the refrigerant vapor inside the hermetic shell, which in turn is affected by heat given off from the motor and compressor, each having

finite efficiency. Because all of these processes are interrelated, they are solved iteratively in the residential version.

In the automobile version, the explicit efficiency submodel is simplified by the fact that the suction and discharge valve ports of an open compressor are not distinguished energetically from the compressor entrance and exit. The isentropic efficiency is therefore interpreted as the "total" efficiency of the overall compressor. As a result, the exiting enthalpy is calculated immediately without requiring any iteration.

Three other major modifications have been made to the model during development of the automobile version. First, the thermal efficiency is calculated in the revised manner discussed previously for the map-based model. Second, the pressure drop in the suction line is now calculated using a subroutine that incorporates the effects of two-phase flow, when the quality is less than unity. This routine was already part of the residential version of the map-based model, but it had never been included in the explicit efficiency submodel. Finally, the mass calculations were changed to omit consideration of the volume inside the hermetic compressor. Variable declarations, common blocks, and WRITE statements have been changed in accordance with these modifications.

Evaporator and Condenser Blowers

To understand the code changes relating to how the blower speed and power are calculated, it is instructive to first outline the options in the residential version. These are complicated. A rather complete outline is presented here for this purpose, and also as a supplement to the residential version documentation (Rice 1991) for those who wish to model hermetic systems.

1. Calculation of cfm:

The residential version requires the user to make use of the following equation:

$$\text{cfm} = \text{cfm}_{\text{ref}} \cdot [\text{rpm}/\text{rpm}_{\text{ref}}] \quad (\text{A-1})$$

Actually, the user must input a reference alternating current frequency, and an actual frequency. These are immediately converted to rpms. For this discussion, we shall refer only to rpms.

2. Calculation of Power

Electric motor power is calculated in the residential version in one of two ways. The following equation may be considered as a "first principles" approach:

$$W_{\text{mot}} = [(\text{cfm} \cdot \Delta P) / \eta_{\text{fan}}] [1 / \eta_{\text{mot/drive}}] \quad (\text{A-2})$$

An alternate approach utilizes the fan laws, which apply for most distribution systems:

$$W_{\text{mot}} = W_{\text{ref}} \cdot (\text{cfm} / \text{cfm}_{\text{ref}})^3 (\rho/\rho_{\text{ref}}) [\eta_{\text{mot/drive,ref}} / \eta_{\text{mot/drive}}] \quad (\text{A-3})$$

Regarding the parameters appearing on the rhs in Eqs. (A-2) and (A-3), the following options are available to users of the residential heat pump version:

- cfm is always found from Eq. (A-1).
- ΔP is found by calling PDAIR, once cfm is known.
- $\eta_{\text{mot/drive}}$ can either be (a) specified as a constant by the user, or (b) calculated using an encoded function of frequency and drive type.
- η_{fan} can either be (a) specified as a constant by the user, or (b) calculated using an encoded function of cfm and ΔP .

3. Option Combinations for Specifying the Blower

The above options are combined into six different sets. The user must select from one of the six sets by choosing values for the input variables FANEFO, ICHODF, MFANFT and IRFCND.

(A) FANEFO \leq 1.0; ICHODF $<$ 0; MFANFT = 0; [IRFCND not used]

- $\eta_{\text{mot/drive}}$ —constant.
- η_{fan} —constant. (Actually, when both are constant, the user specifies FANEFO = $\eta_{\text{mot/drive}} \times \eta_{\text{fan}}$).
- W_{mot} —calculated using Eq. (A-2).

(B) FANEFO \leq 1.0; ICHODF $<$ 0; MFANFT = 1; [IRFCND not used]

- $\eta_{\text{mot/drive}}$ —constant (=FANEFO).
- η_{fan} —calculated using an encoded function of cfm and ΔP .
- W_{mot} —calculated using Eq. (A-2).

(C) FANEFO \leq 1.0; ICHODF \geq 0; MFANFT = 0; [IRFCND not used]

- $\eta_{\text{mot/drive}}$ —calculated using an encoded function of frequency and drive type.
- η_{fan} —constant (=FANEFO).
- W_{mot} —calculated using Eq. (A-2).

(D) FANEFO \leq 1.0; ICHODF \geq 0; MFANFT = 1; [IRFCND not used]

- $\eta_{\text{mot/drive}}$ —calculated using an encoded function of frequency and drive type.
- η_{fan} —calculated using an encoded function of cfm and ΔP .
- W_{mot} —calculated using Eq. (A-2).

(E) FANEFO $>$ 1.0; ICHODF \geq 0; IRFCND \geq 0; [MFANFT not used]

- $\eta_{\text{mot/drive}}$ —calculated using an encoded function of frequency and drive type.
- $\eta_{\text{mot/drive,ref}}$ —calculated using an encoded function of frequency and drive type.
- W_{mot} —calculated using W_{ref} (=FANEFO) in conjunction with $\eta_{\text{mot/drive}}$ and $\eta_{\text{mot/drive,ref}}$ in Eq. (A-3). Here note that W_{ref} is the power of a “reference” drive

type delivering cfm_{ref} at rpm_{ref} . The concept is introduced in order to investigate alternate fan drives for a given fan.

(F) $\text{FANEFO} > 1.0$; $\text{ICHODF} < 0$; $\text{IRFCND} < 0$; [MFANFT not used]

- $\eta_{\text{mot/drive}}$ —assumed equal to $\eta_{\text{mot/drive,ref}}$
- W_{mot} —calculated using W_{ref} (=FANEFO) in conjunction with $\eta_{\text{mot/drive}}$ and $\eta_{\text{mot/drive,ref}}$ in Eq. (A-3).

4. Automobile version

We are now able to describe the blower options that are incorporated into the AHPM.

Condenser: Equation (A-1) is not valid for a system whose pressure drop characteristics are variable. This includes the engine compartment fan that operates against a pressure differential that is a strong function of road speed. For the time being, users of the automobile version will specify a constant cfm (which can be varied parametrically, of course). This choice was simple to implement into the code. If the logical variable OPEN equals "true," then the user specifies only cfm_{ref} . Within the code, rpm is set equal to rpm_{ref} in Eq. (A-1), and cfm equal to cfm_{ref} .

W_{mot} is treated as a constant. The user inputs a constant value, which is assigned to W_{ref} and option (F) is utilized with Eq. (A-3). FANEFO, ICHODF and IRFCND are set automatically as shown in (F), while all three ratios in Eq. (A-3) are assigned to unity. Most of these default parameter values for choosing evaporator and condenser blower options are assigned in DATAIN.

Evaporator: For the indoor blower, the user may select either the option described for the condenser, or option (A). In the latter case, ΔP is calculated in PDAIR and is made up of the coil pressure drop plus a single, constant duct system pressure drop specified by the user. This option has been included so that by varying the duct system resistance parametrically, users may study the effect that evaporator plenum design has on the system performance.

A.2 OVERVIEW OF PLATE-FIN EVAPORATOR: "PLATE" = .TRUE.

The basic solution method for the AHPM evaporator submodel is similar to that for the residential heat pump version (Fischer and Rice 1983). The submodel checks to see if the exiting air temperature is below the dew point temperature. If so, then the fin depth at which condensation first begins is calculated. In the area of the evaporator where dehumidification occurs, the effectiveness/thermal units method is replaced by an "effective surface temperature" approach in which the heat transferred from the air stream is assumed to be proportional to the enthalpy difference between the free stream air and the air at the fin surface (see McElgin and Wiley 1940). The fin efficiency and the fin surface temperature of the wetted fin must be found as part of the solution through iteration, because they in turn depend upon the dehumidification rate.

Although the basic solution method of the residential version was retained, significant modifications were made in order to simulate the "plate-fin" style of heat exchanger used in automotive systems. The mathematical correlations used for calculating the single- and two-phase pressure drop and the single-phase heat transfer were obtained from work by

Lovich and Carey (1990) and Cohen and Carey (1989) for cross-ribbed channel geometry shown in Fig. 2. This geometry is very similar to that used in many Harrison Radiator evaporators and in many Japanese models. Correlations for two-phase boiling heat transfer were obtained from the work of Kandlikar (1991). Air-side correlations for louvered corrugated fins were selected from studies by Davenport (1981). All these correlations are of a generalized form so that the AHPM user can specify the geometry of the evaporator to considerable detail (see Sect. 6).

A.3 LISTING OF QUALITATIVE CHANGES

BLOCK assigns default values to many "common block" variables. The logical variable "OPEN" is assigned here.

DATAIN reads the input data file. If (OPEN) then:

- Compressor volume, used in mass calculations, is set equal to 0. The user does not enter a value for open compressors.
- Coefficients for calculating thermal efficiency explicitly are now read (see D.1).
- Parameters related to the operation of the electric compressor motor and drive are not read.
- All of the default parameter values described above for choosing evaporator and condenser blower options are actually assigned in **DATAIN**.
- Options for adding compressor waste heat to the heat exchanger air streams have been deleted.

The logical variable "PLATE" is read here. If (PLATE) then:

- All geometric parameters for specifying plate-fin evaporators are read in and converted to English units.

PDAIR calculates the air side pressure drops. If (OPEN) then:

- The flow resistance of the filters and supplemental heaters are omitted from the system pressure drop calculations.

If (PLATE) then:

- The air side pressure drop through the plate-fin coil is calculated using empirical correlations obtained from Kays and London (1974). Coefficients for their louvered fin number 3/16-11.1 were also used.
- The increase in coil pressure drop due to accumulation of condensing water on the evaporator fins is modeled using a constant augmentation factor. The relation for finned-tube coils using several fin geometry variables is omitted.

HX converts "indoor" and "outdoor" heat exchanger variables read from the input data file into "evaporator" and "condenser" variables, according to the heat pump mode. If (PLATE) then:

- Variable plate-fin variables are assigned to evaporator variables.

CALC calculates the non-dimensional variables required for the effectiveness-NTU heat exchanger performance methodology. If (PLATE) then:

- A complete new set of relations calculates the eff-NTU variables using the plate-fin geometry variables.

EVAPR is the main subroutine for calculating evaporator performance. If (PLATE) then:

- Defines new air and refrigerant Reynolds numbers.
- Calculates coefficients required for the new 2-phase heat transfer coefficient calculations
- Controls calls to new heat transfer and pressure drop subroutines listed below.
- Omits refrigerant pressure drop in return bends and other ancillary components not relevant to plate-fin configurations.

EVAP accepts heat transfer coefficients and other variables from EVAPR and calculates heat exchanger performance. If (PLATE) then:

- Calculates overall heat transfer coefficient UA using appropriate plate-fin geometry factors.
- Calls new subroutines.

SPHTC2 computes single phase heat transfer coefficients for refrigerant flow. If (PLATE) then:

- Uses new empirical correlations for plate-fin configuration developed by Cohen & Carey (1989).

EHTC calculates two-phase heat transfer coefficients for refrigerant flow. If (PLATE) then:

- Uses new empirical correlations for plate-fin configuration developed by Kandlikar (1991).
- Obtains average value by integrating along the channel length: constant heat flux (linearly increasing quality) is assumed.

HAIR computes air side heat transfer coefficients. If (PLATE) then:

- Uses new correlations developed by Davenport (1981) for louvered, corrugated fins.

SEFF calculates fin efficiency. If (PLATE) then:

- Uses new analytical expression from Kays and London (1974), along with geometric variables relevant to plate-fin design.

PDROP calculates the refrigerant side pressure drop in the evaporator. If (Plate) then:

- Friction component to pressure drop is calculated from empirical correlations for pressure gradient by Lovich and Carey (1990). Integration used for total pressure drop assumes constant heat flux.
- Revised calculation of momentum component of pressure drop for plate-fin geometry.

SUMPRT prints some output parameters. It has been changed according to the above changes to the code.

CMPMAP: See description in A.1.

COMP: See description in A.1.

EPR: See description in Sect. 3.5.

...the ... of ...

...the ... of ...

...the ... of ...

...the ... of ...

...the ... of ...

...the ... of ...

...the ... of ...

...the ... of ...

Appendix B
INPUT AND OUTPUT FILES FOR COMPRESSOR
CURVE-FITTING PROGRAM

1950年10月1日
中华人民共和国中央人民政府
公告

Input Data Definitions and Format

In this appendix, the input data file used for calculating a least-squares fit to the manufacturer's compressor performance curves is given in annotated form. A brief description of each of the input variables is given, along with instructions on how the input file must be formatted. An sample of the input file "MAPIN" is given in the form that is actually used by the program "MAPFIT."

Sample Output Files

This section contains two sample output files, "MAPOUT" and "COEFFS." "MAPOUT" provides the user with the opportunity to examine in detail how well the empirical (biquadratic) curves succeed in approximating the manufacturer's data. "COEFFS" contains the compressor curve-fit coefficients, written in exactly the format required for constructing the "HPDATA" file that was described in Appendix A. This output file can be imported into an existing heat pump model data set with minimal editing.

B.1 INPUT DATA DEFINITIONS AND FORMAT

<u>Variable name</u>	<u>Variable description</u>	<u>Columns</u>
GENERAL DATA:		
<u>Line #1</u>		
NRPM	Number of RPMs for which compressor-data curve-fits are available	[1-10]
MPOW	=0, to indicate that power data are input in HP. =1, to indicate that power data are input in watts. =2, to indicate that power data are input in kilowatts.	[11-20]
MCAP	=1, to identify data as capacity (kBTU/hr). =2, to identify data as mass flow rate (lbm/hr).	[21-30]
NR	Refrigerant number—12, 22, 114, 502, or 134 (If NR is omitted, the default is R12)	[41-50]

COMPRESSOR POWER DATA

(Each of the following variables is given repeatedly for each compressor speed.)

Line #2

Title Descriptive name of the compressor being represented. [1-80]

Line #3

RPMVAL Compressor speed (rpm)[31-40]

DISPLB Displacement of the compressor that is represented in the map (cu. in.)(9.8) [21-30]

SUPER Superheat value for compressor map; [1-10]
 ≥ 0 , base superheat entering compressor ($^{\circ}\text{F}$),
 < 0 , negative of return gas temperature into compressor

SUBCL Refrigerant subcooling (or quality) at the condenser exit [11-20]
for the compressor represented by the map. (*For negative
of the desired quality fraction.)

Line #4

NTCOND Number of condensing temperatures represented by the data. [1-10]

NTEVAP Number of evaporating temperatures represented by the data. [11-20]

Line #5

TSATC The saturation temperatures of the discharge gas ($^{\circ}\text{F}$); [1-10]
There are NTCOND of these temperature values. [11-20]
They should be given in order of increasing temperature. [21-30]
[31-40]
[41-50]
[51-60]

TSATE The saturation temperatures of the compressor inlet gas ($^{\circ}\text{F}$); [1-10]
there are NTEVAP of these temperature values. [11-20]
They should be given in order of increasing temperature. [21-30]
[31-40]
[41-50]
[51-60]

Line #6

CPOWER Compressor power data (hp or Watts or kilowatts). [1-10]
Start with the smallest value of TSATC and enter the power [11-20]
corresponding to each TSATE value. Repeat for each sequentially [21-30]

increasing TSATC value. Altogether, enter NTCOMP \times NTEVAP values. Use as many lines as necessary with six values per line.

[31-40]
[41-50]
[51-60]
[1-10]

WGHT1 Corresponding curve fitting weighting factors for each map data point. Altogether, enter NTCOMP \times NTEVAP values. Use as many lines as necessary with six values per line.

[1-10]
[11-20]
[21-30]
[31-40]
[41-50]
[51-60]
[1-10]

COMPRESSOR MASS FLOW RATE OR CAPACITY

Line #7

Title Title for the mass flow rate (or capacity) data to follow. [1-80]

Line #8

RPMVAL Compressor speed (rpm) [31-40]

DISPLB Displacement of the compressor that is represented in the map (cu. in.) [21-30]

SUPER Superheat value for compressor map;
 ≥ 0 , base superheat entering compressor ($^{\circ}$ F),
 < 0 , negative of return gas temperature into compressor [1-10]

SUBCL Refrigerant subcooling (or quality) at the condenser exit for the compressor represented by the map. ($^{\circ}$ F or negative of the desired quality fraction.) [11-20]

Line #9

NTCOND Number of condensing temperatures represented by the data. [1-10]

NTEVAP Number of evaporating temperatures represented by the data. [11-20]

Line #10

TSATC The saturation temperatures of the discharge gas; There are NTCOND of these temperature values. They should be given in order of increasing temperature.

[1-10]
[11-20]
[21-30]
[31-40]
[41-50]
[51-60]

TSATE The saturation temperatures of the compressor inlet gas; [1-10]
 There are NTEVAP of these temperature values. [11-20]
 They should be given in order of increasing temperature. [21-30]
 [31-40]
 [41-50]

Line #11 [51-60]

XMR or CAPACITY

Mass flow rate (XMR, in lbm/h) or capacity (in kBTU/h). [1-10]
 Start with the smallest value of TSATC and enter the values [11-20]
 corresponding to each TSATE value in order of increasing [21-30]
 TSATE values. Repeat for each sequentially increasing TSATC [31-40]
 value. Altogether, enter NTCOMP \times NTEVAP values. [41-50]
 Use as many lines as necessary with six values per line. [51-60]
 [1-10]

WGHT2 Corresponding curve fitting weighting factors for each map [1-10]
 data point. Altogether, enter NTCOMP \times NTEVAP values. Use [11-20]
 as many lines as necessary with six values per line. [21-30]
 [31-40]
 [41-50]
 [51-60]
 [1-10]

****REPEAT LINES 2 THROUGH 11 FOR EACH RPM VALUE****

B.2 SAMPLE OUTPUT FILES FROM COMPRESSOR CURVE-FITTING PROGRAM

TECHUMSEH HR980: POWER

INPUT DATA FOR MAP COMPRESSOR POWER CONSUMPTION: (HP)

MAP SUPERHEAT VALUE -65.00 F
 MAP SUBCOOLING VALUE 15.00 F
 COMPRESSOR DISPLACEMENT 9.8000 CU IN
 COMPRESSOR MOTOR SPEED 1000. RPM

	EVAPORATING TEMPERATURE (F)	CONDENSING TEMPERATURE (F)				
		130.00	141.00	152.00	161.50	170.00
0 20.0 I DATA	1.4000	1.3000	1.5500	1.6500	1.8000	
I WEIGHT	1.0000	1.0000	1.0000	1.0000	1.0000	
0 30.0 I DATA	1.6000	1.6000	1.8000	1.8500	2.0000	
I WEIGHT	1.0000	1.0000	1.0000	1.0000	1.0000	
0 40.0 I DATA	1.8000	1.9500	2.0000	2.1500	2.3000	
I WEIGHT	1.0000	1.0000	1.0000	1.0000	1.0000	
0 50.0 I DATA	2.0000	2.2000	2.4000	2.5000	2.7500	
I WEIGHT	1.0000	1.0000	1.0000	1.0000	1.0000	

TECHUMSEH HR980: MASS FLOW RATE

INPUT DATA FOR REFRIGERANT MASS FLOW RATE:

MAP SUPERHEAT VALUE -65.00 F
 MAP SUBCOOLING VALUE 15.00 F
 COMPRESSOR DISPLACEMENT 9.8000 CU IN
 COMPRESSOR MOTOR SPEED 1000. RPM

	EVAPORATING TEMPERATURE (F)	CONDENSING TEMPERATURE (F)				
		130.00	141.00	152.00	161.50	170.00
0 20.0 I DATA	210.0000	170.0000	140.0000	120.0000	110.0000	
I WEIGHT	1.0000	1.0000	1.0000	1.0000	1.0000	
0 30.0 I DATA	280.0000	240.0000	210.0000	190.0000	170.0000	
I WEIGHT	1.0000	1.0000	1.0000	1.0000	1.0000	
0 40.0 I DATA	355.0000	310.0000	280.0000	260.0000	240.0000	
I WEIGHT	1.0000	1.0000	1.0000	1.0000	1.0000	
0 50.0 I DATA	420.0000	380.0000	340.0000	320.0000	310.0000	
I WEIGHT	1.0000	1.0000	1.0000	1.0000	1.0000	

TECHUMSEH HR980: POWER

POWER CONSUMPTION (HP)

COEFFICIENTS FOR BI-QUADRATIC FIT:

$$F(X,Y) = 1.6897E-04 * X * X + -4.5225E-02 * X + 2.5000E-04 * Y * Y + -2.1779E-02 * Y + 2.1126E-04 * X * Y + 4.1818E+00$$

	EVAPORATING TEMPERATURE (F)	CONDENSING TEMPERATURE (F)				
		130.00	141.00	152.00	161.50	170.00
0 20.0 I FIT	1.3717	1.4244	1.5180	1.6317	1.7593	
I MAP	1.4000	1.3000	1.5500	1.6500	1.8000	
I %	-2.0217	9.5679	-2.0672	-1.1103	-2.2621	
0 30.0 I FIT	1.5535	1.6295	1.7463	1.8801	2.0256	
I MAP	1.6000	1.6000	1.8000	1.8500	2.0000	
I %	-2.9035	1.8417	-2.9843	1.6256	1.2817	
0 40.0 I FIT	1.7854	1.8846	2.0246	2.1785	2.3420	
I MAP	1.8000	1.9500	2.0000	2.1500	2.3000	
I %	-.8117	-3.3563	1.2303	1.3241	1.8254	

0 50.0 I FIT	2.0672	2.1896	2.3529	2.5269	2.7083
I MAP	2.0000	2.2000	2.4000	2.5000	2.7500
I %	3.3618	-.4710	-1.9613	1.0744	-1.5151

THE MAXIMUM % VARIATION FROM THE MAP VALUE 9.5679
 THE WEIGHTED AVERAGE OF THE ABSOLUTE VALUES OF THE % VARIATIONS 2.2299
 THE WEIGHTED AVERAGE OF THE % VARIATIONS .0834
 THE STANDARD DEVIATION FROM THE AVERAGE % VARIATION 2.9777

1

TECHUMSEH HR980: MASS FLOW RATE
 OMASS FLOW RATE (LB/H)
 COEFFICIENTS FOR BI-QUADRATIC FIT:

$$F(X,Y) = 3.4630E-02*X*X + -1.2738E+01*X + -7.5000E-03*Y*Y + 8.8868E+00*Y + -1.0151E-02*X*Y + 1.1320E+03$$

	CONDENSING TEMPERATURE (F)				
	130.00	141.00	152.00	161.50	170.00
0 20.0 I FIT	209.6861	170.5711	139.8363	120.0367	107.6196
I MAP	210.0000	170.0000	140.0000	120.0000	110.0000
I %	-.1495	.3359	-.1170	.0306	-2.1640
0 30.0 I FIT	281.6078	241.3761	209.5247	188.7608	175.4809
I MAP	280.0000	240.0000	210.0000	190.0000	170.0000
I %	.5742	.5734	-.2263	-.6522	3.2240
0 40.0 I FIT	352.0293	310.6811	277.7130	255.9848	241.8420
I MAP	355.0000	310.0000	280.0000	260.0000	240.0000
I %	-.8368	.2197	-.8168	-1.5443	.7675
0 50.0 I FIT	420.9508	378.4860	344.4013	321.7088	306.7032
I MAP	420.0000	380.0000	340.0000	320.0000	310.0000
I %	.2264	-.3984	1.2945	.5340	-1.0635

THE MAXIMUM % VARIATION FROM THE MAP VALUE 3.2240
 THE WEIGHTED AVERAGE OF THE ABSOLUTE VALUES OF THE % VARIATIONS .7874
 THE WEIGHTED AVERAGE OF THE % VARIATIONS -.0094
 THE STANDARD DEVIATION FROM THE AVERAGE % VARIATION 1.1251

TECHUMSEH HR980: POWER
 INPUT DATA FOR MAP COMPRESSOR POWER CONSUMPTION: (HP)
 MAP SUPERHEAT VALUE -65.00 F
 MAP SUBCOOLING VALUE 15.00 F
 COMPRESSOR DISPLACEMENT 9.8000 CU IN
 COMPRESSOR MOTOR SPEED 2000. RPM

	CONDENSING TEMPERATURE (F)				
	130.00	141.00	152.00	161.50	170.00
0 20.0 I DATA	2.4500	2.6000	2.8000	3.1000	3.4000
I WEIGHT	1.0000	1.0000	1.0000	1.0000	1.0000
0 30.0 I DATA	3.0000	3.1500	3.4000	3.6500	4.0000
I WEIGHT	1.0000	1.0000	1.0000	1.0000	1.0000
0 40.0 I DATA	3.7500	3.9000	4.1500	4.3000	4.6000
I WEIGHT	1.0000	1.0000	1.0000	1.0000	1.0000
0 50.0 I DATA	4.3500	4.7500	5.2000	5.1000	5.2000
I WEIGHT	1.0000	1.0000	1.0000	1.0000	1.0000

TECHUMSEH HR980: MASS FLOW RATE
 INPUT DATA FOR REFRIGERANT MASS FLOW RATE:

MAP SUPERHEAT VALUE -65.00 F
 MAP SUBCOOLING VALUE 15.00 F
 COMPRESSOR DISPLACEMENT 9.8000 CU IN
 COMPRESSOR MOTOR SPEED 2000. RPM

EVAPORATING TEMPERATURE (F)	CONDENSING TEMPERATURE (F)				
	130.00	141.00	152.00	161.50	170.00
0 20.0 I DATA	335.0000	300.0000	280.0000	250.0000	220.0000
I WEIGHT	1.0000	1.0000	1.0000	1.0000	1.0000
0 30.0 I DATA	445.0000	400.0000	370.0000	340.0000	320.0000
I WEIGHT	1.0000	1.0000	1.0000	1.0000	1.0000
0 40.0 I DATA	560.0000	510.0000	480.0000	450.0000	430.0000
I WEIGHT	1.0000	1.0000	1.0000	1.0000	1.0000
0 50.0 I DATA	670.0000	630.0000	610.0000	560.0000	530.0000
I WEIGHT	1.0000	1.0000	1.0000	1.0000	1.0000

1

TECHUMSEH HR980: POWER
 OPOWER CONSUMPTION (HP)
 COEFFICIENTS FOR BI-QUADRATIC FIT:

$$F(X,Y) = 7.2393E-05 * X * X + 4.9903E-03 * X + 5.2500E-04 * Y * Y + 4.9994E-02 * Y + -1.2090E-04 * X * Y + -3.9367E-01$$

EVAPORATING TEMPERATURE (F)	CONDENSING TEMPERATURE (F)				
	130.00	141.00	152.00	161.50	170.00
0 20.0 I FIT	2.3741	2.6182	2.8798	3.1198	3.3457
I MAP	2.4500	2.6000	2.8000	3.1000	3.4000
I %	-3.0995	.6985	2.8493	.6394	-1.5979
0 30.0 I FIT	2.9793	3.2101	3.4585	3.6870	3.9026
I MAP	3.0000	3.1500	3.4000	3.6500	4.0000
I %	-.6889	1.9089	1.7191	1.0139	-2.4355
0 40.0 I FIT	3.6896	3.9071	4.1421	4.3592	4.5645
I MAP	3.7500	3.9000	4.1500	4.3000	4.6000
I %	-1.6106	.1821	-.1899	1.3765	-.7720
0 50.0 I FIT	4.5049	4.7091	4.9308	5.1364	5.3314
I MAP	4.3500	4.7500	5.2000	5.1000	5.2000
I %	3.5602	-.8617	-5.1771	.7132	2.5268

THE MAXIMUM % VARIATION FROM THE MAP VALUE 5.1771
 THE WEIGHTED AVERAGE OF THE ABSOLUTE VALUES OF THE % VARIATIONS 1.6811
 THE WEIGHTED AVERAGE OF THE % VARIATIONS .0377
 THE STANDARD DEVIATION FROM THE AVERAGE % VARIATION 2.1454

1

TECHUMSEH HR980: MASS FLOW RATE
 OMASS FLOW RATE (LB/H)
 COEFFICIENTS FOR BI-QUADRATIC FIT:

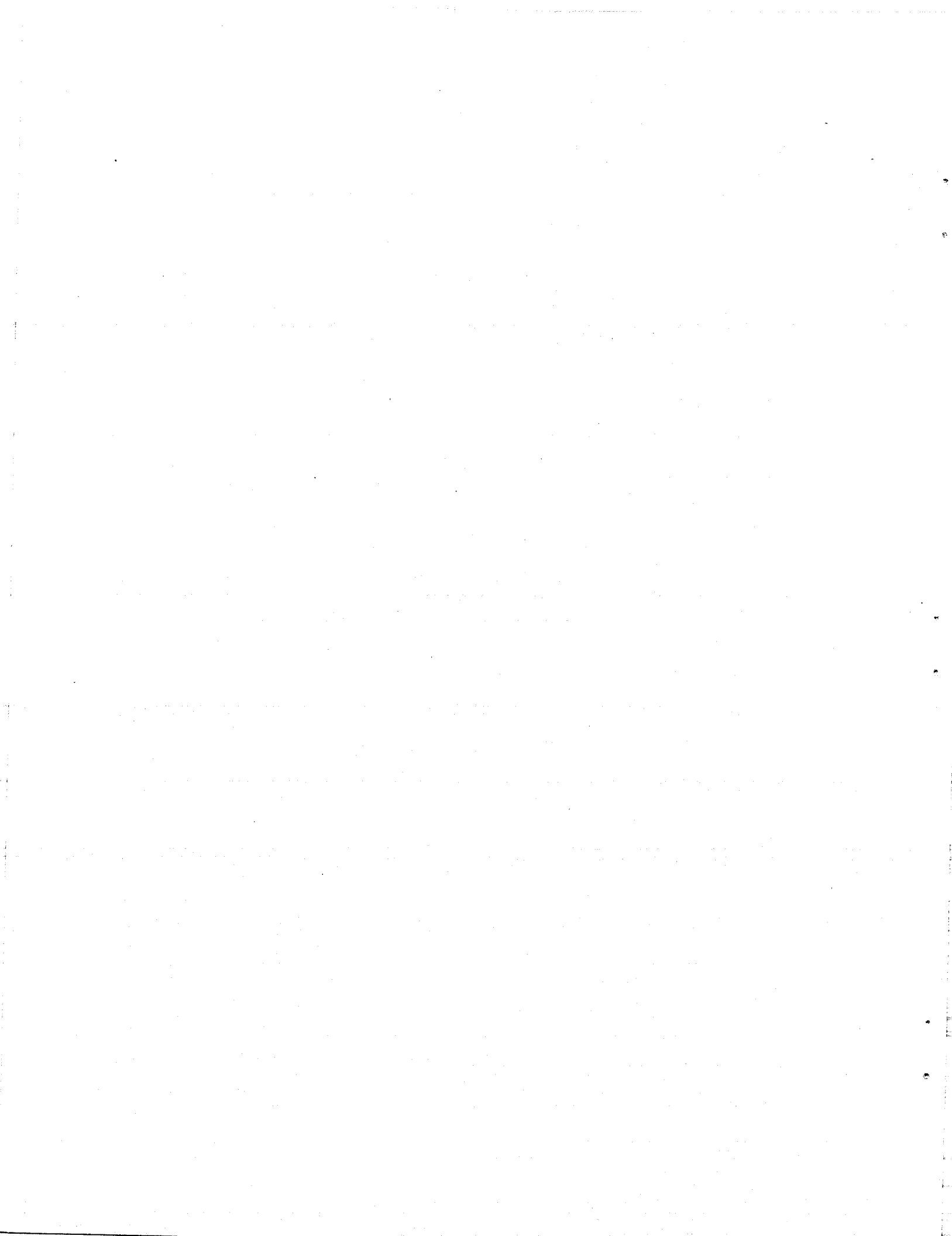
$$F(X,Y) = 3.9567E-03 * X * X + -3.5605E+00 * X + 4.0000E-02 * Y * Y + 1.1277E+01 * Y + -2.1713E-02 * X * Y + 5.4688E+02$$

EVAPORATING TEMPERATURE (F)	CONDENSING TEMPERATURE (F)				
	130.00	141.00	152.00	161.50	170.00
0 20.0 I FIT	335.9593	303.8120	272.6223	246.4563	223.6500
I MAP	335.0000	300.0000	280.0000	250.0000	220.0000
I %	.2863	1.2707	-2.6349	-1.4175	1.6591
0 30.0 I FIT	440.4973	405.9616	372.3835	344.1547	319.5028
I MAP	445.0000	400.0000	370.0000	340.0000	320.0000

I %	-1.0118	1.4904	.6442	1.2220	-.1554
0 40.0 I FIT	553.0355	516.1113	480.1446	449.8531	423.3555
I MAP	560.0000	510.0000	480.0000	450.0000	430.0000
I %	-1.2437	1.1983	.0301	-.0326	-1.5452
0 50.0 I FIT	673.5735	634.2609	595.9058	563.5515	535.2083
I MAP	670.0000	630.0000	610.0000	560.0000	530.0000
I %	.5334	.6763	-2.3105	.6342	.9827

THE MAXIMUM % VARIATION FROM THE MAP VALUE	2.6349
THE WEIGHTED AVERAGE OF THE ABSOLUTE VALUES OF THE % VARIATIONS	1.0490
THE WEIGHTED AVERAGE OF THE % VARIATIONS	.0138
THE STANDARD DEVIATION FROM THE AVERAGE % VARIATION	1.2855

APPENDIX C
SAMPLE AUTOMOBILE HEAT PUMP MODEL OUTPUT



***** CONTOUR DATA GENERATION INFORMATION *****
 0*** CONTOUR DATA GENERATOR FRONT-END IS BYPASSED ***
 1
 0***** INPUT DATA *****

VARIABLE-SPEED AIR CONDITIONER; PLATE-FIN EVAPORATOR; 30 MPH.

SUMMARY OUTPUT
 COOLING MODE OF OPERATION
 THE REFRIGERANT IS R 12

REFRIGERANT MASS INVENTORY OMITTED

REFRIGERANT CHARGE IS NOT SPECIFIED

COMPRESSOR INLET SUPERHEAT IS SPECIFIED AT 10.00 F
 0 CONDENSER EXIT SUBCOOLING IS SPECIFIED AT 16.00 F
 0 ESTIMATE OF:
 SATURATION TEMPERATURE INTO COMPRESSOR 37.40 F
 SATURATION TEMPERATURE OUT OF COMPRESSOR 155.00 F
 0 MECHANICAL EFFICIENCY OF COMPRESSOR IS .900
 0 COMPRESSOR CHARACTERISTICS:
 OPERATING ROTATION RATE 2000.000
 TOTAL DISPLACEMENT 9.800 CUBIC INCHES
 0 TECHUMSEH HR980 COMPRESSOR:
 0 RETURN GAS TEMPERATURE FOR COMPRESSOR MAP 65.000 F
 BASE DISPLACEMENT FOR COMPRESSOR MAP 9.800 CU IN
 1

***** INPUT DATA *****

0 -- USER PROVIDED COEFFICIENTS FOR COMPRESSOR POWER AND MASS FLOW RATE AT DISCRETE FREQUENCIES --
 0 CURVE FIT REPRESENTATIONS AT 5 DISCRETE RPM VALUES
 0 CURVE FIT COEFFICIENTS AT NOMINAL SPEED OF 1000.0 RPM
 POWER CONSUMPTION= 1.690E-04*CONDENSING TEMPERATURE**2 + -4.523E-02*CONDENSING TEMPERATURE
 + 2.500E-04*EVAPORATING TEMPERATURE**2 + -2.178E-02*EVAPORATING TEMPERATURE
 + 2.113E-04*CONDENSING TEMPERATURE*EVAPORATING TEMPERATURE + 4.182E+00 HP
 MASS FLOW RATE= 3.463E-02*CONDENSING TEMPERATURE**2 + -1.274E+01*CONDENSING TEMPERATURE
 + -7.500E-03*EVAPORATING TEMPERATURE**2 + 8.887E+00*EVAPORATING TEMPERATURE
 + -1.015E-02*CONDENSING TEMPERATURE*EVAPORATING TEMPERATURE + 1.132E+03 LBM/HR
 0 CURVE FIT COEFFICIENTS AT NOMINAL SPEED OF 2000.0 RPM
 POWER CONSUMPTION= 7.239E-05*CONDENSING TEMPERATURE**2 + 4.990E-03*CONDENSING TEMPERATURE
 + 5.250E-04*EVAPORATING TEMPERATURE**2 + 4.999E-02*EVAPORATING TEMPERATURE
 + -1.209E-04*CONDENSING TEMPERATURE*EVAPORATING TEMPERATURE + -3.937E-01 HP
 MASS FLOW RATE= 3.957E-03*CONDENSING TEMPERATURE**2 + -3.560E+00*CONDENSING TEMPERATURE
 + 4.000E-02*EVAPORATING TEMPERATURE**2 + 1.128E+01*EVAPORATING TEMPERATURE
 + -2.171E-02*CONDENSING TEMPERATURE*EVAPORATING TEMPERATURE + 5.469E+02 LBM/HR
 0 CURVE FIT COEFFICIENTS AT NOMINAL SPEED OF 3000.0 RPM
 POWER CONSUMPTION= -1.796E-04*CONDENSING TEMPERATURE**2 + 9.979E-02*CONDENSING TEMPERATURE
 + 6.000E-04*EVAPORATING TEMPERATURE**2 + 1.530E-01*EVAPORATING TEMPERATURE
 + -6.193E-04*CONDENSING TEMPERATURE*EVAPORATING TEMPERATURE + -8.402E+00 HP
 MASS FLOW RATE= -3.215E-02*CONDENSING TEMPERATURE**2 + 6.782E+00*CONDENSING TEMPERATURE
 + 8.750E-02*EVAPORATING TEMPERATURE**2 + 1.124E+01*EVAPORATING TEMPERATURE
 + -2.028E-02*CONDENSING TEMPERATURE*EVAPORATING TEMPERATURE + -1.062E+02 LBM/HR
 0 CURVE FIT COEFFICIENTS AT NOMINAL SPEED OF 4000.0 RPM
 POWER CONSUMPTION= -3.594E-04*CONDENSING TEMPERATURE**2 + 1.678E-01*CONDENSING TEMPERATURE
 + 7.500E-04*EVAPORATING TEMPERATURE**2 + 2.314E-01*EVAPORATING TEMPERATURE
 + -9.974E-04*CONDENSING TEMPERATURE*EVAPORATING TEMPERATURE + -1.416E+01 HP
 MASS FLOW RATE= -6.521E-02*CONDENSING TEMPERATURE**2 + 1.682E+01*CONDENSING TEMPERATURE

+ 1.025E-01*EVAPORATING TEMPERATURE**2 + 1.460E+01*EVAPORATING TEMPERATURE
 + -2.907E-02*CONDENSING TEMPERATURE*EVAPORATING TEMPERATURE + -8.267E+02 LBM/HR
 0 CURVE FIT COEFFICIENTS AT NOMINAL SPEED OF 5000.0 RPM
 POWER CONSUMPTION= -5.441E-04*CONDENSING TEMPERATURE**2 + 2.381E-01*CONDENSING TEMPERATURE
 + 9.000E-04*EVAPORATING TEMPERATURE**2 + 3.258E-01*EVAPORATING TEMPERATURE
 + -1.502E-03*CONDENSING TEMPERATURE*EVAPORATING TEMPERATURE + -2.023E+01 HP
 MASS FLOW RATE= -8.410E-02*CONDENSING TEMPERATURE**2 + 2.225E+01*CONDENSING TEMPERATURE
 + 1.325E-01*EVAPORATING TEMPERATURE**2 + 1.599E+01*EVAPORATING TEMPERATURE
 + -3.220E-02*CONDENSING TEMPERATURE*EVAPORATING TEMPERATURE + -1.179E+03 LBM/HR
 0 SUPERHEAT CORRECTION TERMS (SET IN BLOCK DATA):
 SUCTION GAS HEATING FACTOR .330
 VOLUMETRIC EFFICIENCY CORRECTION FACTOR .750
 SUCTION SUPERHEAT HEAT TRANSFER FACTOR .050
 SUCTION GAS HEAT PICKUP FRACTION .750
 1

***** INPUT DATA *****

0 INDOOR UNIT:
 INLET AIR TEMPERATURE 85.000 F RELATIVE HUMIDITY .52000
 AIRFLOW RATE 175.00 CFM
 NOMINAL FAN POWER 148.00 WATTS
 FRONTAL AREA OF HX .520 SQ FT PLATE-FIN HEAT EXCHANGER
 LENGTH OF AIR CHANNELS 72.00 MM FIN PITCH 14.00 FINS/IN
 NUMBER OF PARELLEL CIRCUITS 4.33 FIN THICKNESS .00600 IN
 PLATE HEIGHT 1.80000 MM LOUVER LENGTH IN FLOW DIRECTION 1.16700 MM
 GAP BETWEEN PLATES 9.25000 MM THERMAL CONDUCTIVITY: FINS 95.00 BTU/H-FT-F
 PLATE THICKNESS .700 MM THERMAL CONDUCTIVITY: PLATES 95.00 BTU/H-FT-F
 DISTANCE BETWEEN RIBS 10.700 MM REF-SIDE HEAT-TRANSFER MULTIPLIER 1.00000
 RIB ANGLE 45.000 DEG AIR-SIDE HEAT-TRANSFER MULTIPLIER 1.00000
 RIB WIDTH 3.100 MM REF-SIDE PRESSURE DROP MULTIPLIER 1.00000
 AIR-SIDE PRESSURE DROP MULTIPLIER-UNIT 1.00000
 AIR-SIDE PRESSURE DROP MULTIPLIER-SYSTEM 1.00000

0 OUTDOOR UNIT:
 INLET AIR TEMPERATURE 95.000 F RELATIVE HUMIDITY .80000
 AIRFLOW RATE 2600.00 CFM
 NOMINAL FAN POWER 110.00 WATTS
 FRONTAL AREA OF HX 3.020 SQ FT GENERAL LOUVERED (SIMPLE-STRIP) FINS
 NUMBER OF TUBES IN DIRECTION OF AIR FLOW 2.00 FIN PITCH 10.00 FINS/IN
 NUMBER OF PARALLEL CIRCUITS 2.00 FIN THICKNESS .00600 IN
 OD OF TUBES IN HX .37500 IN THERMAL CONDUCTIVITY: FINS 95.00 BTU/H-FT-F
 ID OF TUBES IN HX .32500 IN THERMAL CONDUCTIVITY: TUBES 95.00 BTU/H-FT-F
 HORIZONTAL TUBE SPACING .720 IN FRACTION OF COMPUTED CONTACT CONDUCTANCE 999.000
 VERTICAL TUBE SPACING 1.000 IN NUMBER OF RETURN BENDS 32.00
 REF-SIDE HEAT-TRANSFER MULTIPLIER 1.000 AIR-SIDE HEAT-TRANSFER MULTIPLIER 1.000
 REF-SIDE PRESSURE-DROP MULTIPLIER 1.000 AIR-SIDE PRESSURE-DROP MULTIPLIER - UNIT 1.000
 AIR-SIDE PRESSURE-DROP MULTIPLIER - SYSTEM 1.000

***** INPUT DATA *****

0 LINE HEAT TRANSFER:
 HEAT GAIN IN SUCTION LINE 100.0 BTU/H
 HEAT LOSS IN DISCHARGE LINE 100.0 BTU/H
 HEAT LOSS IN LIQUID LINE 100.0 BTU/H
 0 DESCRIPTION OF CONNECTING TUBING:
 LIQUID LINE FROM INDOOR TO OUTDOOR HEAT EXCHANGER
 ID .25550 IN
 EQUIVALENT LENGTH 39.80 FT

FROM INDOOR COIL TO REVERSING VALVE
 ID .68600 IN
 EQUIVALENT LENGTH 31.00 FT
 FROM REVERSING VALVE TO COMPRESSOR INLET
 ID .79300 IN
 EQUIVALENT LENGTH 5.00 FT

FROM OUTDOOR COIL TO REVERSING VALVE
 ID .68600 IN
 EQUIVALENT LENGTH 2.00 FT
 FROM REVERSING VALVE TO COMPRESSOR OUTLET
 ID .56100 IN
 EQUIVALENT LENGTH 2.00 FT

0 ITERATION TOLERANCES :

AMBCON	.050 F	CMPCON	.050 BTU/LBM	TOLH	.00050 BTU/LBM
CNDCON	.050 F	FLOCON	.400 F	TOLS	.00003 BTU/LBM-R
EVPCON	.100 F	CONMST	.002 F		

PLATE FIN RESULTS

REFRIGERANT SIDE FREE FLOW AREA PER CIRCUIT .00121
 REF-SIDE HYDRAULIC DIAM. .00794
 AIR-SIDE HYDRAULIC DIAM. .00980
 TOTAL AIR-SIDE HEAT TRANS. AREA PER CIRC. 8.33789
 FACE WIDTH 2.84857

0 CALC: COMPUTED HEAT EXCHANGER CHARACTERISTICS

	CONDENSER	EVAPORATOR
AIR FLOW AREA / FRONTAL AREA	.57622	.65823
INSIDE PERIMETER OF TUBE (FT)	.08508	.00000
OUTSIDE PERIMETER OF TUBE (FT)	.10132	.00000
OUTSIDE CROSS-SECTIONAL AREA OF TUBE (FT2)	.00082	.00000
CROSS-SECTIONAL FLOW AREA OF TUBE (FT2)	.00058	.00000
CONTACT CONDUCTANCE (BTU/H-FT2-F)	*****	.000
LENGTH OF HX TUBING PER CIRCUIT (FT)	36.240	2.849
REFRIGERANT SIDE HEAT TRANSFER AREA PER CIRCUIT (FT2)	3.083	1.737
TOTAL REFRIGERANT SIDE HEAT TRANSFER AREA ALL CIRCUITS (FT2)	6.167	.000
REFRIGERANT SIDE HEAT TRANSFER AREA / HEAT EXCHANGER VOLUME (1/FT)	17.017	61.234
TOTAL AIR-SIDE HEAT TRANSFER AREA (FT2)	79.67	.00
FIN HEAT TRANSFER AREA / TOTAL AIR-SIDE HEAT TRANSFER AREA	.913	.839
AIR SIDE HEAT TRANSFER AREA / HEAT EXCHANGER VOLUME (1/FT)	219.838	293.916
AIR-TO-REFRIGERANT HEAT TRANSFER AREA RATIO	12.919	.000

1

***** CALCULATED HEAT PUMP PERFORMANCE *****

SYSTEM SUMMARY	REFRIGERANT TEMPERATURE	SATURATION TEMPERATURE	REFRIGERANT ENTHALPY	REFRIGERANT QUALITY	REFRIGERANT PRESSURE	AIR TEMPERATURE
COMPRESSOR SUCTION LINE INLET	31.966 F	25.430 F	80.945 BTU/LBM	1.0000	39.629 PSIA	
SHELL INLET	32.866	22.866	81.199	1.0000	37.753	
SHELL OUTLET	158.959	127.376	95.355	1.0000	189.366	
CONDENSER INLET	157.607 F	127.337 F	95.101 BTU/LBM	1.0000	189.271 PSIA	95.000 F
OUTLET	110.149	126.152	33.568	.0000	186.460	103.559
EXPANSION DEVICE	109.112 F	123.877 F	33.314 BTU/LBM	.0000	181.147 PSIA	
EVAPORATOR INLET	31.064 F	31.064 F	33.314 BTU/LBM	.2762	44.000 PSIA	85.000 F

OUTLET 31.966 25.430 80.945 1.0000 39.629 29.479
 OCOMPRESSOR PERFORMANCE

OVERALL EFFICIENCIES
 COMPRESSOR POWER 1.813 KW ISENTROPIC .8082
 COMPRESSOR SPEED 2000.000 RPM VOLUMETRIC .6198
 MECHANICAL .9000 AT A PRESSURE RATIO OF 5.016
 0 REFRIGERANT MASS FLOW RATE 393.492 LBM/H
 OFAN/BLOWER PERFORMANCE CONDENSER EVAPORATOR
 AIR FLOW RATE 2600.00 CFM 175.00 CFM
 FACE VELOCITY 860.93 FT/MIN 336.54 FT/MIN
 SURFACE VELOCITY 1494.09 FT/MIN 511.28 FT/MIN
 COIL PRESSURE DROP .464 IN H2O .008 IN H2O

***** CALCULATED HEAT PUMP PERFORMANCE *****

CONDENSER -- HEAT TRANSFER PERFORMANCE OF EACH CIRCUIT

INLET AIR TEMPERATURE 95.000 F
 OUTLET AIR TEMPERATURE 103.559 F
 0 TOTAL HEAT EXCHANGER EFFECTIVENESS .3064
 0 SUPERHEATED TWO-PHASE SUBCOOLED
 REGION REGION REGION
 NTU .0000 .3539 .7832
 HEAT EXCHANGER EFFECTIVENESS 1.0000 .2980 .5143
 CR/CA .0000 .2243
 FRACTION OF HEAT EXCHANGER .0000 .8450 .1550
 HEAT TRANSFER RATE .0 BTU/H 11317.1 BTU/H 788.9 BTU/H
 0 OUTLET AIR TEMPERATURE 95.000 F 104.469 F 98.598 F
 AIR SIDE: REFRIGERANT SIDE:
 MASS FLOW RATE 5580.4 LBM/H MASS FLOW RATE 196.7 LBM/H
 PRESSURE DROP .4643 IN H2O PRESSURE DROP 2.811 PSI
 AUGMENTATION FACTOR 2.031 HEAT TRANSFER COEFFICIENT
 HEAT TRANSFER VAPOR REGION 130.463 BTU/H-SQ FT-F
 COEFFICIENT 26.318 BTU/H-SQ FT-F TWO PHASE REGION 477.564 BTU/H-SQ FT-F
 AUGMENTATION FACTOR 1.750 SUBCOOLED REGION 119.890 BTU/H-SQ FT-F
 0 CONTACT INTERFACE:
 CONTACT CONDUCTANCE 923846.900 BTU/H-SQ FT-F
 UA VALUES PER CIRCUIT:
 VAPOR REGION (BTU/H-F) TWO PHASE REGION (BTU/H-F) SUBCOOLED REGION (BTU/H-F)
 REFRIGERANT SIDE .000 REFRIGERANT SIDE 1244.300 REFRIGERANT SIDE 57.303
 AIR SIDE .000 AIR SIDE 644.787 AIR SIDE 118.281
 CONTACT INTERFACE .000 CONTACT INTERFACE 100886.400 CONTACT INTERFACE 18506.800
 COMBINED .000 COMBINED 422.927 COMBINED 38.521

OFLOW CONTROL DEVICE -- CONDENSER EXIT SUBCOOLING IS SPECIFIED AS 16.000 F

CORRESPONDING TXV RATING PARAMETERS: CORRESPONDING CAPILLARY TUBE PARAMETERS: CORRESPONDING ORIFICE PARAMETER:
 RATED OPERATING SUPERHEAT 11.000 F NUMBER OF CAPILLARY TUBES 1 ORIFICE DIAMETER .0636 IN
 STATIC SUPERHEAT RATING 6.000 F CAPILLARY TUBE FLOW FACTOR 4.187
 PERMANENT BLEED FACTOR 1.150
 FRACTION OF RATED OPENING .107
 TXV CAPACITY RATING: 5.967 TONS
 WITH NOZZLE AND TUBES

***** CALCULATED HEAT PUMP PERFORMANCE *****

EVAPORATOR -- HEAT TRANSFER PERFORMANCE OF EACH CIRCUIT

	INLET AIR TEMPERATURE	85.000 F		
	OUTLET AIR TEMPERATURE	29.479 F		
0	MOISTURE REMOVAL OCCURS			
0	SUMMARY OF DEHUMIDIFICATION PERFORMANCE (TWO-PHASE REGION)			
0		LEADING EDGE	POINT WHERE MOISTURE	
		OF COIL	REMOVAL BEGINS	LEAVING EDGE OF COIL
		AIR	AIR	AIR
			WALL	WALL
	DRY BULB TEMPERATURE	85.000 F	85.000 F	35.834 F
	HUMIDITY RATIO	.01340	.01340	.00440
	ENTHALPY	35.159 BTU/LBM	35.159 BTU/LBM	13.355 BTU/LBM
0	RATE OF MOISTURE REMOVAL			1.7803 LBM/H
	FRACTION OF EVAPORATOR THAT IS WET			1.0000
	LATENT HEAT TRANSFER RATE IN TWO-PHASE REGION			1873. BTU/H
	SENSIBLE HEAT TRANSFER RATE IN TWO-PHASE REGION			2366. BTU/H
	SENSIBLE TO TOTAL HEAT TRANSFER RATIO FOR TWO-PHASE REGION			.5582
	OVERALL SENSIBLE TO TOTAL HEAT TRANSFER RATIO			.5582
0	OVERALL CONDITIONS ACROSS COIL			
		ENTERING	EXITING	
		AIR	AIR	
	DRY BULB TEMPERATURE	85.000 F	29.479 F	
	WET BULB TEMPERATURE	71.203 F	29.356 F	
	RELATIVE HUMIDITY	.520	.990	
	HUMIDITY RATIO	.01340	.00332	
0	TOTAL HEAT EXCHANGER EFFECTIVENESS (SENSIBLE)			.9708
0		SUPERHEATED	TWO-PHASE	
		REGION	REGION	
	NTU	2.2099	3.6810	
	HEAT EXCHANGER EFFECTIVENESS	.8755	.9748	
	CR/CA	14.5415		
	FRACTION OF HEAT EXCHANGER	.0221	.9779	
	HEAT TRANSFER RATE	89.8 BTU/H	4238.8 BTU/H	
	AIR MASS FLOW RATE	3.90 LBM/H	172.77 LBM/H	
	OUTLET AIR TEMPERATURE	32.925 F	29.401 F	
0	AIR SIDE:		REFRIGERANT SIDE:	
	MASS FLOW RATE	176.7 LBM/H	MASS FLOW RATE	90.9 LBM/H
	PRESSURE DROP	.158 IN H2O	PRESSURE DROP	4.370 PSI
	AUGMENTATION FACTOR	1.000		
	HEAT TRANSFER COEFFICIENT		HEAT TRANSFER COEFFICIENT	
	DRY COIL	21.212 BTU/H-SQ FT-F	VAPOR REGION	130.746 BTU/H-SQ FT-F
	WET COIL	23.899 BTU/H-SQ FT-F	TWO PHASE REGION	2322.144 BTU/H-SQ FT-F
	AUGMENTATION FACTOR	1.000		
0	CONTACT INTERFACE:			
	CONTACT CONDUCTANCE	.000 BTU/H-SQ FT-F		
	DRY FIN EFFICIENCY	.947		
	WET FIN EFFICIENCY (AVERAGE)	.907		
	WET CONTACT FACTOR (AVERAGE)	1.330		
0	UA VALUES PER CIRCUIT:VAPOR			
		REGION	REGION	
	REFRIGERANT SIDE	5.012	3944.783 BTU/H-F	
	AIR SIDE			
	DRY COIL	3.695	.000 BTU/H-F	
	WET COIL		176.770 BTU/H-F	
	CONTACT INTERFACE			
	DRY COIL	1585.608	.000 BTU/H-F	
	WET COIL		70270.730 BTU/H-F	
	COMBINED			

DRY COIL	2.124	.000 BTU/H-F
WET COIL		168.782 BTU/H-F

1
 0***** SUMMARY OF ENERGY INPUT AND OUTPUT *****

0 VARIABLE-SPEED AIR CONDITIONER; PLATE-FIN EVAPORATOR; 30 MPH.

0 OPERATING CONDITIONS:

AIR TEMPERATURE INTO EVAPORATOR	85.00 F
AIR TEMPERATURE INTO CONDENSER	95.00 F
SATURATION TEMP INTO COMPRESSOR	22.87 F
SATURATION TEMP OUT OF COMPRESSOR	127.38 F

0 ENERGY INPUT SUMMARY:

HEAT PUMPED FROM AIR SOURCE	18742.7 BTU/H
POWER TO INDOOR FAN MOTOR	148.0 WATTS
POWER TO OUTDOOR FAN MOTOR	110.0 WATTS
TOTAL PARASITIC POWER	258.0 WATTS

POWER TO COMPRESSOR	1813.4 WATTS
TOTAL POWER TO COMPRESSOR AND FANS	2071.4 WATTS

0 REFRIGERANT-SIDE SUMMARY:

HEAT GAIN TO EVAPORATOR FROM AIR	18742.7 BTU/H
HEAT GAIN TO SUCTION LINE	100.0 BTU/H
ENERGY INPUT TO COMPRESSOR	6189.1 BTU/H
HEAT LOSS FROM COMPRESSOR SHELL	618.9 BTU/H
HEAT LOSS FROM DISCHARGE LINE	100.0 BTU/H
HEAT LOSS FROM CONDENSER TO AIR	24212.0 BTU/H
HEAT LOSS FROM LIQUID LINE	100.0 BTU/H

0 ENERGY OUTPUT SUMMARY:

HEAT RATE FROM REFRIGERANT TO INDOOR AIR	18742.7 BTU/H
TOTAL HEAT RATE TO/FROM INDOOR AIR	18742.7 BTU/H

0 COOLING PERFORMANCE:

COP	2.651
EER	9.048 BTU/H-W
CAPACITY	18742.7 BTU/H

APPENDIX D
DEFINITIONS OF CONSTANTS ASSIGNED IN BLOCK DATA

THE UNIVERSITY OF CHICAGO

A number of variables and constants are used by the Heat Pump Design Model that are unlikely to be changed often; consequently, they are simply assigned values rather than being specified with each set of input data. They have been brought together in the BLOCK DATA subroutine and given values that are in turn passed to the subroutines where they are used via common blocks. These data are divided into several categories organized by function.

Assignment of Unit Numbers for Input and Output

Input Unit Numbers

IOCHZR for reading "CONCHZ" and "HPDATA" data files, 5
IOCNTN for reading "CONTRL" data files (optional), 24

Output Unit Numbers

IOCONW for printing the input echo and the output listing, 6
IOSSP for punching a steady-state performance data file of the form required for the ORNL Annual Performance Factor Model, 7
IOCONP for punching contour data files "CONGEN" or "CONSPD" (from Figure CDG1), 8

Physical Air-Side Parameters

PA atmospheric pressure, 14.7 lbf/in²
RAU universal gas constant, 53.34 ft-lbf/lbm-°R
AFILTR flow area of filter on indoor unit, 2.78 ft²
AHEATR cross-sectional area of resistance heater section in indoor unit, (usually equal to indoor blower exit area), 1.28 ft²
RACKS number of resistance heater racks, 3.0

Data for Choosing Open or Hermetic Compressors

OPEN If .TRUE. then program models an open compressor.
 If .FALSE. then program models a closed compressor.

Data For Loss-and-Efficiency-Based Compressor Model

Compressor Motor Efficiency Correlation

CETAM coefficients for the 0th through 5th order terms of the fit of the compressor motor efficiency as a function of the fractional motor load (Eq. 4.29*), 0.4088, 2.5138, -4.6289, 4.5884, -2.3666, and 0.48324

* The equation numbers cited throughout the BLOCK DATA variable definitions refer to a previous ORNL Heat Pump Model documentation report (Fischer and Rice 1983).

RPMSLR slope of linear fit for fraction of no-load compressor motor speed as a function of fraction of full load power, -0.042 (see Eq. 4.24*)

Compressor Volumetric Efficiency Parameters

ETA VLA intercept for the fit of theoretical minus actual volumetric efficiencies as a linear function of the correlating parameter given by Davis and Scott, -0.0933
ETA VLB slope of the fit of theoretical minus actual volumetric efficiencies as a linear function of the correlating parameter given by Davis and Scott, 0.733

Data For Map-Based Compressor Model

Shell Inlet Superheat Correction Parameters

SUCFAC suction gas heating factor F_{sh} used in Eq. 4.6*, 0.33
VOLFAC volumetric efficiency correction factor F_v used in Eq. 4.4*, 0.75

Parameters for Converting Between Induction and ECM Compressor Motors

CSLPNM assumed nominal compressor slip speed at rated horsepower for the selected drive, 150 rpm
NPINDC number of poles for compressor induction motor, 2
MPOLCM multiplier to convert number of induction motor poles to number of poles for compressor ECM, 2

Factors For Estimating Suction Gas Superheat Effects Of Different Motors

LOCOOL logical variable used to omit suction gas superheat corrections if motor is not low-side cooled, $.TRUE.$
HTFRAC estimated fraction of the shaft input power that contributes to suction gas heating, 0.05
DAMPER damping factor on total suction gas heating from motor cooling and from heat transfer from the compressor body and discharge line, 0.75

PM-ECM Motor Characteristics (Used for Motor Temperature Corrections)

ETSTAT estimate of motor stator temperature, 40.0°C
ETROTR estimate of motor rotor temperature, 55.0°C
ETREF reference temperature for motor data, 25.0°C
ETCOEF magnet flux temperature coefficient ($-0.20\% / ^\circ\text{C}$)
EFORMF approximate average form factor, 1.01
ESPDNM(J) motor nominal speed (rpm), $5400., 6900.$
ETQRAT(J) rating point (design cooling load) torque (oz-ft), $64.0, 50.0$
ERTREF(J) motor stator resistance (line-line) at reference temperature (ohms), $0.648, 0.371$
EACOE(J) slope of torque/current relationship, $0.205, 0.263$
EBCOE(J) intercept of torque/current relationship, $0.6, 0.3$
where $(I = A * T + B)$ for two motor speeds $J = 1, 2$
which provide 2 points from which to interpolate to other nominal speeds

Fan and Fan Motor Parameters

Data for Outdoor Fan Efficiency Representation

COFAN	constant term for the fit of outdoor fan static efficiency to fan specific speed, -3.993
CIFAN	coefficient for the linear term of the fit of outdoor fan static efficiency to the fan specific speed, 4.266
C2FAN	coefficient for the quadratic term of the fit of outdoor fan static efficiency to fan specific speed, -1.024

Fan Power Reference Temperatures

TRFIDF(1)	reference temperature for indoor fan power in <i>cooling</i> mode,	80.0°F
TRFIDF(2)	reference temperature for indoor fan power in <i>heating</i> mode,	70.0°F
TRFODF(1)	reference temperature for outdoor fan power in <i>cooling</i> mode,	95.0°F
TRFODF(2)	reference temperature for outdoor fan power in <i>heating</i> mode,	47.0°F

Parameters for Converting Between Induction and ECM Fan Motors

SLPNMI	indoor-blower assumed nominal slip speed at rated horsepower, 120 rpm
SLPNMI	outdoor-fan assumed nominal slip speed at rated horsepower, 120 rpm
NPOLEI	number of poles for indoor-blower induction motor, 6
NPOLEO	number of poles for outdoor-fan induction motor, 6
MPOLEI	multiplier to convert number of induction motor poles to number of poles for indoor-blower ECM, 2
MPOLEO	multiplier to convert number of induction motor poles to number of poles for outdoor-fan ECM, 2

Iteration Convergence Criteria (Default Values)

AMBCON	Convergence parameter for the iteration on evaporator inlet air temperature, 0.20°F
CNDCON	Convergence parameter for the iteration on condenser exit subcooling (or on exit quality * 200)—used when IREFC = 0 on Line 6 (°F); also the quantity {2 * CNDCON} is used as the convergence parameter for the charge balancing iteration when ICHRG = 2, 0.20°F
FLOCON	Convergence parameter for iteration on refrigerant mass flow rate—used when IREFC > 0 on Line 6 (equivalent F°) value is specified as if it were in degrees F and is scaled internally (by 1/20 th) to give a mass flow convergence factor, 0.20°F
EVPCON	Convergence parameter for iteration on evaporator exit superheat (or on exit quality 500); Also the quantity {2 EVPCON} is used as the convergence parameter for the charge balancing iteration when ICHRG = 1, 0.50 F°
CONMST	Convergence parameter for iterations on evaporator tube wall temperatures in subroutine EVAP and dew-point temperature in subroutine XMOIST, 0.003°F

Iteration Convergence Criteria (continued)

CMPCON	Convergence parameter for iteration on suction gas enthalpy in the efficiency-and-loss compressor model (Btu/lbm)—only used when ICOMP = 1 on Line 8, 0.05 °F
TOLH	Tolerance parameter used by refrigerant routines in calculating properties of superheated vapor when converging on a known <i>enthalpy</i> value (Btu/lbm), 0.001
TOLS	Tolerance parameter used by refrigerant routines in calculating properties of superheated vapor when converging on a known <i>entropy</i> value (Btu/lbm/°R), 0.00005

Refrigerant Specification (Default)

NR refrigerant number, 22

Refrigerant-Side Heat Transfer Correlation for Condenser Vapor Region

C1R, C3R, and C5R	coefficients for single-phase heat transfer coefficient (Eq. 6.2*), 1.10647, 3.5194×10^{-7} , and 0.01080
C2R, C4R, and C6R	exponents for single-phase heat transfer coefficient (Eq. 6.3*), -0.78992, 1.03804, and -0.13750
XLLR	lower limit on the Reynolds number for laminar flow of refrigerant, 3,500
ULR	upper limit for the Reynolds number for turbulent flow of refrigerant, 6,000

Refrigerant Tubing Parameter

E roughness of interior tube walls, 5×10^{-6} ft

Evaporator Dryout Criterion

XDO refrigerant quality at which dryout occurs in the evaporator, 0.75

Refrigerant Flow Control Parameters

Thermostatic Expansion Valve Constants (Set for R22 as Default)

BLEEDF	bypass or bleed factor coefficient used to compute TXV parameters when condenser subcooling is held fixed, 1.15
DPRAT	rated pressure drop across the TXV at the design conditions, 100 psi for R-22 and R-502, 60 psi for R-12
NZTBOP	switch to bypass nozzle and distributor tube pressure drop calculations when calculating TXV parameters if the condenser subcooling is held fixed, 0
STATIC	static superheat setting used to compute the TXV parameters when the condenser subcooling is held fixed, 6.0 °F
SUPRAT	rated operating superheat used to compute the TXV parameters when the condenser subcooling is held fixed, 11.0 °F
TERAT	rated evaporating temperature for the TXV, 40.0 °F

TLQRAT rated liquid refrigerant temperature at the inlet to the TXV, 100.0°F
XLTUBE length of distributor tubes (if used), 30 in.

Capillary Tube Parameter

NCAP number of capillary tubes used to compute capillary tube flow factor, ϕ , when
condenser subcooling is held fixed, 1.

1947

...

...

...

...

...

...

...

INTERNAL DISTRIBUTION

- | | |
|--------------------|---------------------------------|
| 1. R. S. Carlsmith | 10. R. B. Shelton |
| 2. F. C. Chen | 11. A. W. Trivelpiece |
| 3. G. E. Courville | 12. W. R. Wilburn |
| 4. W. Fulkerson | 13. Central Research Library |
| 5. P. S. Gillis | 14. Document Reference Section |
| 6. M. A. Kuliasha | 15-16. Laboratory Records Dept. |
| 7. D. M. Kyle | 17. Laboratory Records - RC |
| 8. V. C. Mei | 18. ORNL Patent Office |
| 9. C. K. Rice | |

EXTERNAL DISTRIBUTION

19. Anthony W. Abraham, PE, Director, Strategic Planning, Wynn's Climate Systems, Inc., 1900 SE Loop 820, P.O. Box 40870, Fort Worth, Texas 76140-0870
20. Eugene C. Boyer, Executive Vice President, Technology, Hayden, 1531 Pomona Road, P.O. Box 848, Corona, California 91718-0848
21. John Burgers, Long Manufacturing, Ltd., 656 Kerr Street, Oakville, Ontario L6K 3E4, CANADA
22. Samuel Chen, Project Engineer, Calsonic Technical Center, 10232 South 51st Street, Phoenix, Arizona 85044
23. Z. George Chen, Test/Analysis Engineer, Thermal Components, Inc., 2760 Gunter Park Drive, West, Montgomery, Alabama 36109
24. Alan R. Christ, Program Manager, Bus Manufacturing U.S.A., Inc., 325-F Rutherford Avenue, Goleta, California 93117
25. Dr. Richard N. Christensen, Professor, Department of Mechanical Engineering, Nuclear Engineering Program, The Ohio State University, 206 West 18th Avenue, Columbus, Ohio 43210-1107
26. Refki Elbourini, Manager, Project Engineering, Calsonic Technical Center, 10232 South 51st Street, Phoenix, Arizona 85044
27. Kevin D. Funke, Engineer, Department 602, John Deere Dubuque Works, 18600 South John Deere Road, P.O. Box 538, Dubuque, Iowa 52001
28. Richard A. Good, Product Manager, Hydro Aluminum Bohn, P.O. Box 5083, Southfield, Michigan 48037
29. Rial E. Hamann, Engineering Specialist, Systems & Applications, McCord Heat Transfer Corporation, 850 Ladd Road, P.O. Box 700, Walled Lake, Michigan 48390-3026
30. Dr. Doyoung Han, Associate Professor, Department of Mechanical Engineering, Kook Min University, 861-1, Jeoungneung-Dong, Seoungbuk-Ku, Seoul, 136, KOREA
31. R. T. Holmes, Director, Mecelec Developments Limited, Llanthony Road, Gloucester, GL1 5QT, ENGLAND
32. Dr. Lawrence R. Hudson, Senior Project Manager, New York State Energy Research and Development Authority, 2 Rockefeller Road, Albany, New York 12223
33. Dr. Ronald O. Hultgren, Deputy Assistant Manager, Department of Energy, Oak Ridge Operations, Post Office Box 2008, Oak Ridge, Tennessee 37831-6269

34. Robert Janezich, Engineering Department, L&M Radiator, Inc., 1414 East 37th Street, Hibbing, Minnesota 55746
35. Michael Kauffeld, Development, Heat Transfer Tønder a.s., Postbox 50, Hydrovej 6, DK-6270 Tønder, DENMARK
36. Peter Li, Engineering and Research Staff, Control Systems Department, Ford, P.O. Box 2053, Dearborn, Michigan 48121
37. Peter G. Malone, Principal R&D Engineer, Air Conditioning Controls, Automotive and Appliance Controls Division, Eaton Corporation, 191 East North Avenue, Carol Stream, Illinois 60188-2090
38. Roberto Mancina, Box 02-5255, POBA # 352, Miami, Florida 33102-5255
39. Arthur A. Naujock, Climate Control and I/P Systems Specialist, Body Engineering, Liberty & Technical Affairs - Vehicle Engineering, Chrysler Corporation, 30900 Stephenson Highway, Madison Heights, Michigan 48071
- 40-41. Office of Scientific and Technical Information, Post Office Box 62, Oak Ridge, Tennessee 37831
42. S. Ohba, President, Soleq Corporation, 5969 North Elston Avenue, Chicago, Illinois 60646
43. David W. Patterson, Chief Engineer, Heat Exchanger Products, Harrison Radiator Division, General Motors Corporation, 200 Upper Mountain Road, A&E Building 6, Lockport, New York, 14094
44. Jostein Pettersen, Research Engineer, Section Refrigeration and Heat Pumps, SINTEF Refrigeration Engineering, N-7034 Trondheim, NORWAY
45. Roy Radcliffe, Sales and Marketing, Tripac World Headquarters, P.O. Box 185638, Fort Worth, Texas 76181
46. Ernie Schumacher, Fujikoki America, Inc., 4040 Bronze Way, Dallas, Texas 75237
47. Rod A. Struss, Senior Research Advisor, Modine Manufacturing Company, 1500 DeKoven Avenue, Racine, Wisconsin 53403
48. David J. Twichell, PE, Senior Research and Development Engineer, Truck Division, Valeo Engine Cooling, 2258 Allen Street, Jamestown, New York 14701-2396
49. Bjørn Vestergaard, Process Engineer, Hydro Aluminum Bohn, Inc., 100 Gus Hipp Boulevard, Rockledge, Florida 32955
50. Evan Waymire, PE, Development Engineer, Freightliner Corporation, 4747 North Channel Avenue, P.O. Box 3849, Portland, Oregon 97208-3849
51. Dr. Peter White, School of Engineering, Coventry University, Priory Street, Coventry, CVI 5FB, UNITED KINGDOM
52. Douglas L. Williams, Vice President and General Manager, Heat Exchange Division, Sanden International (U.S.A.), Inc., 601 South Sanden Boulevard, Wylie, Texas 75098-4999